ChemComm

ROYAL SOCIETY OF CHEMISTRY

FEATURE ARTICLE

View Article Online
View Journal | View Issue

Check for updates

Cite this: *Chem. Commun.*, 2025, **61**, 1104

The coordination chemistry of *p-tert*-butylcalix[8]arene with transition and lanthanide metal ions†

Abhijnan Chakraborty, [a] Lucinda R. B. Wilson, [a] Scott J. Dalgarno *[b] and Euan K. Brechin *[a]

Received 14th October 2024,
Accepted 21st November 2024

DOI: 10.1039/d4cc05459h

rsc.li/chemcomm

A survey of the literature and the Cambridge Structural Database reveals thirty nine *p-tert*-butylcalix[8]arene-supported transition (3d, limited to V–Cu) and lanthanide metal complexes ranging in nuclearity from one to eighteen, twenty of which are homometallic and nineteen of which are heterometallic. We provide a review of the coordination chemistry of these complexes, including our own work in the area. We also provide our thoughts and perspectives on the common structural themes observed, identify gaps in knowledge and evaluate how that may inform and direct future synthetic efforts. What is clear is that the coordination chemistry of H_8TBC[8] with paramagnetic metal ions remains hugely underexplored.

Open Access Article. Published on 22 2024. Downloaded on 31.05.2026 00:39:47.
This article is licensed under a Creative Commons Attribution-NonCommercial 3.0 Unported Licence.

Introduction

Recent years have seen a vast expansion in the coordination chemistry of *p-tert*-butylcalix[4]arene (H_4TBC[4]), particularly in relation to the synthesis of polynuclear 3d, 4f, and 3d–4f clusters that display a range of fascinating physical properties (*e.g.* single molecule magnetism and magnetic refrigeration).[1] The calix[4]arene (C[4]) scaffold is an extremely attractive ligand in this regard as it can be synthesised and modified with relative ease, but also because it is predisposed to bind a series of metal ions in the polyphenolic pocket. Furthermore, the conformational properties of C[4]s are well-understood, particularly when the lower-rim comprises only hydroxyl groups, and these molecules can form cone, partial-cone, 1,2-alternate and 1,3-alternate conformers.[2] These conformations can also be accessed through the introduction of small substituents at the lower-rim (*e.g.* OMe), whilst larger groups can be used to lock out a particular conformer as desired. In most cases, this step would preclude the ability to form polynuclear clusters, so it is not of particular relevance to this review and will not be discussed further. The *p-tert*-butylthia-, sulfonyl- and sulfinylcalix[4]arene analogues have attracted similar interest

[a] *EaStCHEM School of Chemistry, The University of Edinburgh, David Brewster Road, Edinburgh, EH9 3FJ, UK. E-mail: ebrechin@ed.ac.uk*
[b] *Institute of Chemical Sciences, Heriot-Watt University, Riccarton, Edinburgh, EH14 4AS, UK. E-mail: S.J.Dalgarno@hw.ac.uk*

† Electronic supplementary information (ESI) available: Table of compounds in the review and additional figures. See DOI: https://doi.org/10.1039/d4cc05459h

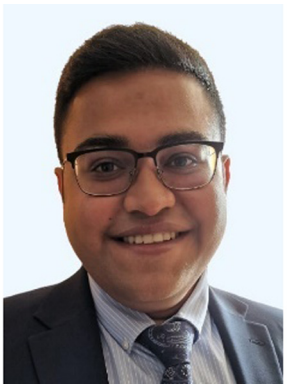

Abhijnan Chakraborty

Abhijnan Chakraborty is currently a 2nd year PhD student in Professor Euan Brechin's group. Originally from India, he obtained his MChem degree from the University of Edinburgh in 2023. His research focuses on exploring the coordination chemistry of calixarenes with various transition metals and lanthanides.

Lucinda R. B. Wilson

Lucinda R. B. Wilson completed both her MChem (2020) and PhD (2024) degrees at The University of Edinburgh, the latter under the supervision of Prof E. K. Brechin. Her PhD research involved exploring the structure–property relationships of calix[n]arene-supported clusters whilst her current post-doctoral research focuses on the synthesis and characterisation of iron-based molecular minerals.

This journal is © The Royal Society of Chemistry 2025

Open Access Article. Published on 22 2024. Downloaded on 31.05.2026 00:39:47.
This article is licensed under a Creative Commons Attribution-NonCommercial 3.0 Unported Licence.

in coordination chemistry, building on the fact that their conformations are equally well understood, but also because a common $[M_4(S^-/SO^-/SO_2{}^-TBC[4])Cl]^{n+}$ (n = 2, 3) metalloligand results that can be exploited in directed assembly.[3] Notably, this metalloligand has been utilised in the formation of a range of spectacular cage structures that have been exploited in areas such as selective guest/gas uptake and sorption.

Some of the larger homologues of H_4TBC[4] are highly desirable for exploring polynuclear cluster formation, an example being H_9TBC[9] which has been seen to adopt a triple-cone conformation akin to a three leaf clover in the solid state upon complexation to lanthanide ions.[4] This molecule would be very interesting for synthesising highly symmetric polyhedra of 3d/4f ions but, as is the case for many of the very large homologues, it is (to our knowledge) only accessible in relatively small amounts *via* laborious synthetic and purification protocols. This therefore hinders the potential utility of the larger H_nTBC[n]s in the synthesis of coordination clusters, with the exception of H_8TBC[8] which can be isolated on a large scale with ease. Indeed, it has often been found to be an unwanted product in calixarene synthesis. One might intuitively expect H_8TBC[8] to behave as two H_4TBC[4]s from a coordination chemistry perspective, but the conformations adopted by the octamer upon coordination, coupled with the methylene bridge orientations, preclude such behaviour. To achieve this effect one must tether two H_4TBC[4]s through a single methylene bridge from each to afford H_8-bis-TBC[4], a ligand that does indeed display augmented coordination chemistry that mimics that of fused C[4]s.[5] It is well known that moving beyond the general C[6] scaffold (*i.e.* $\geq$ C[7]) leads to a large increase in both flexibility and the associated number of possible conformers in the free calixarene. It therefore follows that, although larger H_nTBC[n]s present very exciting opportunities for unearthing new coordination chemistry through favoured coordination modes, there are intrinsic challenges arising from conformational versatility prior to tailoring assembly with such moieties.

A recent paper by Kieliszek and Malinska comprehensively described the various conformations of H_8TBC[8] observed in a range of solvated crystal structures, surveying the Cambridge Structural Database in the process, to provide an excellent overview.[6] A range of intra- and intermolecular interactions are involved in stabilising common conformations observed in the solvates studied, these being chair-loop, chair and pleated-loop (Fig. 1). An excellent early example of how the versatility of H_8TBC[8] can be exploited in host–guest chemistry is its ability to selectively complex C_{60} from a range of fullerenes in soot.[7] In this case, the hosts adopt a double-cone conformation, encapsulating C_{60} molecules to form a complex that can then be harvested in crystalline form and deconstructed to afford pure buckminsterfullerene.

In this article we provide a review of the coordination chemistry of *p-tert*-butylcalix[8]arene with 3d transition (limited to V–Cu) and 4f lanthanide metal ions, including our own work in the area, with an emphasis on prevailing magnetic properties. We also provide our thoughts and perspectives on the common structural themes observed, identify gaps in knowledge and evaluate how that may inform and direct future synthetic efforts. A search of the Cambridge Structural Database (CSD, July 2024) and the literature for *p-tert*-butylcalix[8]arene-supported transition (V–Cu) and lanthanide metal complexes results in 39 hits (Table S1, ESI†).[8–37] Of these, 11 are homometallic 3d complexes, 3 are heterometallic 3d–4/5d complexes, 7 are heterometallic 3d-s complexes, 2 are heterometallic 3d-p complexes, 9 are homometallic 4f complexes, 4 are heterometallic 3d–4f complexes, 2 are heterometallic 3d–5f complexes, and 1 is a heterometallic 4f-s complex. The smallest contains a single metal ion and the largest a total of eighteen metal ions.

V-based clusters

The biggest contributors to this family are polymetallic clusters of V, principally investigated for their catalytic properties.[8–13] The first reported example was the dimer $[RNH_3][V^V{}_2O_2(H_1TBC[8])]$ (**1**), published in 1990.[8] Complex **1** (Fig. 2) was synthesised from the reaction of $[VO(O^iPr)_3]$ with H_8TBC[8] in THF. The core of the complex describes a $[V_2O_2]$ dimer with the two metal ions bridged by two μ-O(Ph) atoms from the hepta-deprotonated H_1TBC[8] ligand. The latter is in

Scott J. Dalgarno

Scott J. Dalgarno is Chair of Supramolecular Chemistry at Heriot-Watt University. His research interests are in self-/metal-directed assembly, crystal engineering, host–guest chemistry and energetic materials. He has been the recipient of the Royal Society of Chemistry Harrison-Meldola Memorial and Sir Edward Frankland prizes, and the Chemical Communications Emerging Investigator Lectureship.

Euan K. Brechin

Euan K. Brechin is the Crum Brown Chair of Chemistry at The University of Edinburgh. His research interests are in synthetic coordination chemistry and molecular magnetism. He has been the recipient of the Royal Society of Chemistry Mond-Nyholm, Tilden, Corday-Morgan and Sir Edward Frankland prizes.

Open Access Article. Published on 22 2024. Downloaded on 31.05.2026 00:39:47.
This article is licensed under a Creative Commons Attribution-NonCommercial 3.0 Unported Licence.

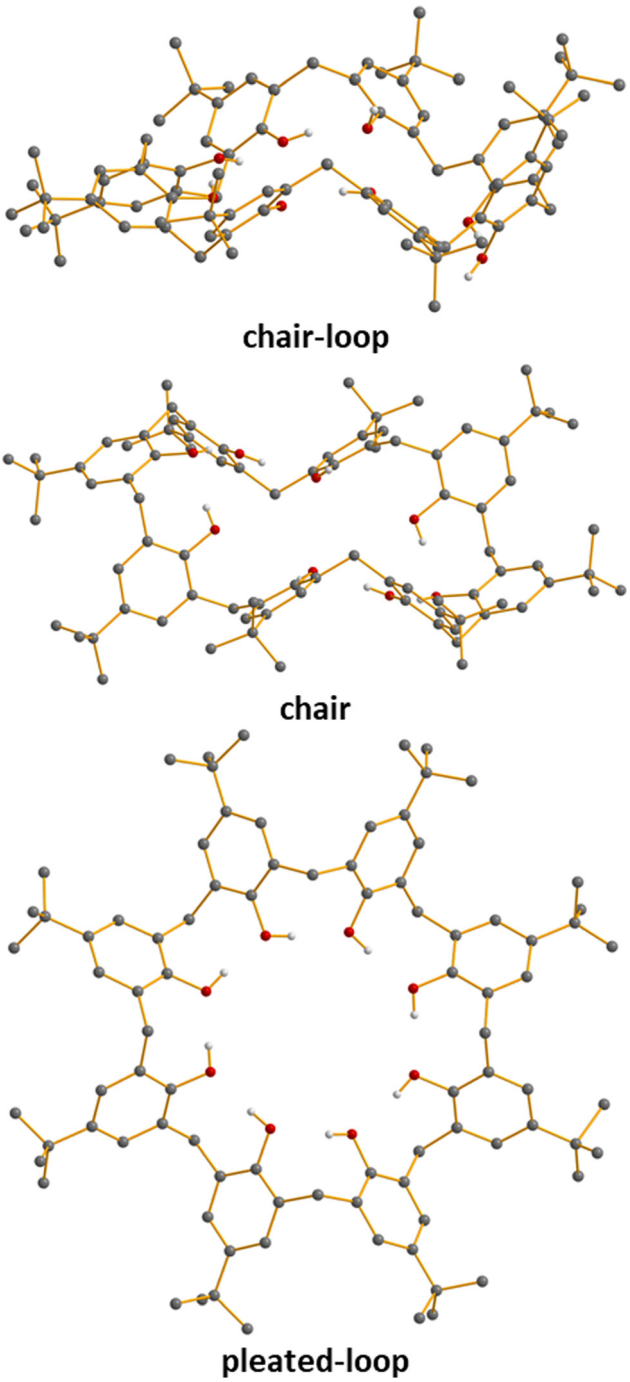

Fig. 1 Common conformations of H_8TBC[8] found in a range of solvates. Chair-loop (top), chair (middle) and pleated-loop (bottom). Colour code: C = grey, O = red, H = white. H(–C) atoms and solvent of crystallisation omitted for clarity.

the 'saddle-shaped' conformation, twisting in such a way as to provide five O-atoms to each octahedral V^V centre, the sixth coordination site on each metal ion being occupied by a terminally bonded oxide (O^{2-}) ion.

The second example, $[V^V_2(p\text{-tolylN})_2(H_2TBC[8])]$ (**2**), reported in 2001,[9] was made from the reaction of $[V(p\text{-tolylN})(O^tBu)_3]$ with H_8TBC[8] in toluene (Fig. S1, ESI†). Its structure is similar

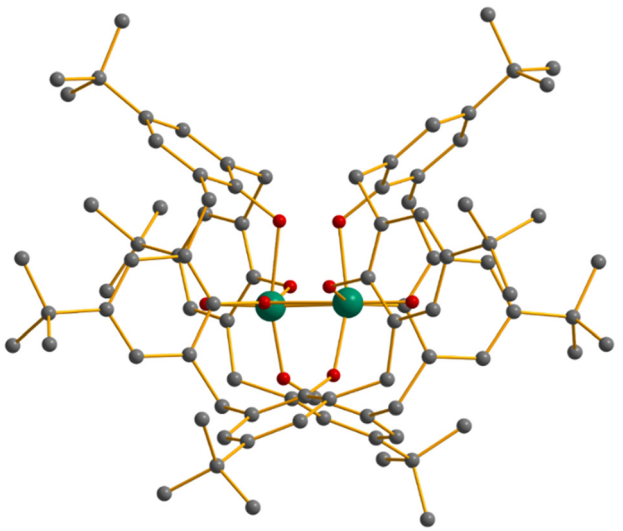

Fig. 2 Structure of the anionic $[V_2]$ dimer in **1**. All reported $[V_2]$ dimers are structurally similar, differing only in the presence of either an O^{2-} or NR^{2-} ion on the sixth coordination site on each V centre. Complexes **1**, **3–6** all contain the calix[8]arene in the hepta-deprotonated H_1TBC[8] form and the complexes are charge balanced by a single cation. Complex **2** contains H_2TBC[8] and is neutral. Colour code: V = dark green, O = red, C = grey. H atoms and counter ions omitted for clarity.

to **1**, but with an organoimido (NR^{2-}) ligand occupying the sixth coordination site on each metal. In this case the calixarene is hexa-deprotonated and the complex is neutral. Four other $[V^V_2]$ dimers are known (Fig. S2 and S3, ESI†), $[PPh_4][V^V_2O_2(H_1TBC[8])]$ (**3**), $[Li(MeCN)_4][V^V_2O_2(H_1TBC[8])]$ (**4**), $[Na(MeCN)_5][V^V_2O_2(H_1TBC[8])]$ (**5**) and $[^tBuNH_3][V^V_2(p\text{-tolylN})_2(H_1TBC[8])]$ (**6**).[10,11] All are structurally similar to **1** and **2**. In each case the sixth coordination site on each V centre is occupied by a terminally bonded O^{2-}/NR^{2-} ion, with the calix[8]arene being hepta-deprotonated and charge balance maintained through the presence of a single cation. Compound **5** is made *via* the reaction of H_8TBC[8] with $[NaVO(O^tBu)_4]$, the latter being formed *in situ* from $VOCl_3$. Increasing the ratio of $[NaVO(O^tBu)_4]$ in the reaction leads to the formation of $[Na(MeCN)_6][V^V_8Na_7O_{16}(TBC[8])_2(MeCN)_6]$ (**7**).[11] The anionic cluster (Fig. 3) sits on an inversion centre, with each half containing four VO_2 moieties bonded to four Na ions, one of which is at half-occupancy. Each of the V ions is four coordinate and in tetrahedral $\{VO_4\}$ geometry. The fully deprotonated TBC[8] ligand adopts a pleated-loop conformation, bonded to the four V ions in the asymmetric unit (ASU). Two neighbouring O(Ph) groups possess μ-bridging O-atoms that serve to link the two halves of the molecule together, bonding to a single V ion in one half and to two Na ions on the other half. Charge balance is maintained through the presence of two half-occupancy $[Na(MeCN)_6]^+$ cations.

The same reaction but employing $[KVO(O^tBu)_4]$ results in the formation of the alkali-metal-free complex $[V^V_4O_6(TBC[8])]$ (**8**; Fig. 4).[11] The metal–oxygen core of **8** describes a near planar $[(VO)_4O_2]$ butterfly, each V ion being five coordinate and in square pyramidal $\{VO_5\}$ geometry. The fully deprotonated

This journal is © The Royal Society of Chemistry 2025

Open Access Article. Published on 22 2024. Downloaded on 31.05.2026 00:39:47.
This article is licensed under a Creative Commons Attribution-NonCommercial 3.0 Unported Licence.

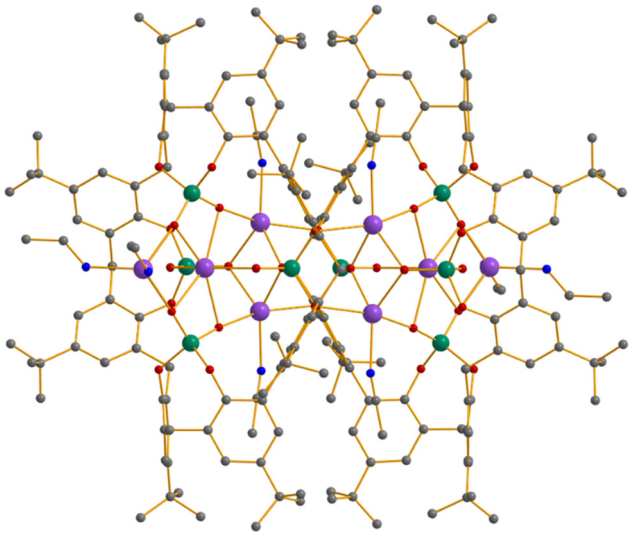

Fig. 3 The structure of the anionic cluster of compound **7**. Colour code: V = dark green, Na = purple, O = red, N = blue, C = grey. H atoms and counter ions omitted for clarity.

TBC[8] ligand adopts a double-cone conformation, lying "above" the $[V_4]$ plane (as drawn in Fig. 4). Two of the eight O(Ph) atoms are μ-bridging across the body-wing edge of the butterfly, while the remaining six are terminally bonded.

Employing LiO^tBu in a reaction with $VOCl_3$ and H_8TBC[8] in THF/Et_2O leads to the isolation of the heterometallic complex $[V^V_4Li_6O_8(TBC[8])(O^tBu)_2(THF)_2(Et_2O)_2]$ (**9**; Fig. S4, ESI†).[11] At the centre of the cluster lies a $[V_4Li_4(\mu_3\text{-}O)_4(\mu\text{-}O)_4]$ cage comprising two fused $[V_2Li_2(\mu_3\text{-}O)_4]$ butterflies, the four μ-bridging O^{2-} ions linking the two halves of the cage together. Each V centre is four coordinate and in tetrahedral $\{VO_4\}$ geometry. Two additional Li ions sit above the cage and are linked to it *via* μ-bridging O^{t}Bu molecules. The calixarene adopts a pseudo-pleated loop conformation, with each neighbouring pair of O(Ph) atoms chelating to a V ion.

The four remaining V-based complexes, and those published most recently, are the isostructural heterometallic tetramers $[V^V_2Nb^V_2O_5(O^iPr)_2(TBC[8])(MeCN)_2]$ (**10**) and $[V^V_2Ta^V_2O_5(O^iPr)_2(TBC[8])(MeCN)_2]$ (**11**; Fig. 5), the hexamer $[V^V_3V^{IV}_1Nb^V_2O_9(O^nPr)_3(TBC[8])(MeCN)_2]$ (**12**; Fig. S5, ESI†) and the monomer $[HNEt_3]_2[V^VO_2(H_5TBC[8])]$ (**13**; Fig. S6, ESI†).[12,13] Complexes **10** and **11** result from the reaction of H_8TBC[8] with $[VO(O^iPr)_3]$ and $[Nb(OEt)_5]$ or $[Ta(OEt)_5]$ in toluene, followed by crystallisation from MeCN. The central core of each complex contains a (bent) V–O–Nb/Ta–O–Nb/Ta–O–V chain. The fully deprotonated TBC[8] ligand is in the pleated-loop conformation, with each neighbouring pair of O(Ph) atoms chelating to either a V or Nb/Ta ion. The V ions are four coordinate and in $\{VO_4\}$ geometries, the fourth site being occupied by a terminally bonded O^{2-} ion. The Nb/Ta ions are six coordinate and in octahedral $\{Nb/TaO_5N_1\}$ geometries, with their fifth and sixth sites being occupied by MeCN and O^{i}Pr molecules.

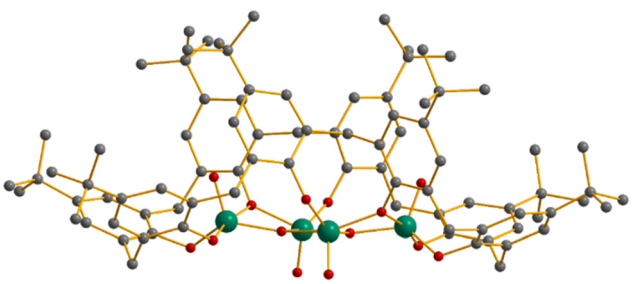

Fig. 4 The structure of compound **8**. Colour code: V = dark green, O = red, C = grey. H atoms omitted for clarity.

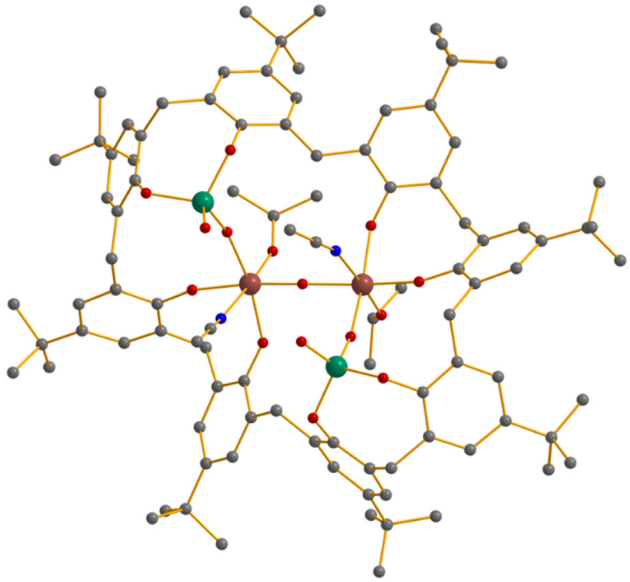

Fig. 5 The structure common to both **10** and **11**. Colour code: V = dark green, Nb/Ta = maroon, O = red, N = blue, C = grey. H atoms omitted for clarity.

Replacing $[VO(O^iPr)_3]$ with $[VO(O^nPr)_3]$ in the same reaction that affords tetrameric complex **10** results in the formation of the hexameric complex **12**.[12] The same central (bent) V–O–Nb/Ta–O–Nb/Ta–O–V chain prevails, but with two additional V ions asymmetrically capping both sides of the Nb–Nb vector, linked by one $\mu_3\text{-}O^{2-}$ ion and two $\mu\text{-}O^{2-}$ ions, respectively. The fully deprotonated TBC[8] ligand coordinates in the same way as in **10** and **11**. The three O^{n}Pr ligands are of two types, two are μ-bridging between neighbouring Nb–V–Nb ions, with the third terminally bonded to the same V ion. The Nb ions are six coordinate and in octahedral $\{NbO_6\}$ geometries. The V ions are of three types, two are four coordinate and in tetrahedral $\{VO_4\}$ geometries, one is five coordinate and in square pyramidal $\{VO_5\}$ geometry, while one is six coordinate and in an octahedral $\{VO_4N_2\}$ geometry with its coordination sphere completed by two MeCN molecules. It is this metal ion that is V^{IV}.

The reaction of $VO(SO_4)$ with H_8TBC[8] and NEt_3 in refluxing MeOH, followed by crystallisation from MeCN, affords complex **13**.[13] The triply deprotonated H_5TBC[8] ligand sits in a pleated-loop conformation, using two of its deprotonated O(Ph) atoms to bond to the single V^V ion, whose tetrahedral geometry is completed by two terminal O^{2-} ions. The latter are H-bonded to the two $HNEt_3$ cations that sit one above and one below the

Open Access Article. Published on 22 2024. Downloaded on 31.05.2026 00:39:47.
This article is licensed under a Creative Commons Attribution-NonCommercial 3.0 Unported Licence.

calix[8]arene plane. The third deprotonated O(Ph) atom lies directly opposite the $\{VO_4\}$ moiety, H-bonding to it two nearest neighbours.

Summary of V-based clusters

From the above, it is clear that the coordination chemistry of vanadium (thus far) is dominated by the V^V ion. There are no examples of homovalent V^{IV} or V^{III} species in the literature, and there is just one mixed valent species. The vast majority of complexes have been synthesised *via* air- and moisture-free techniques in non-protic solvents. Very few, if any, have been made in the presence of air/moisture using standard benchtop techniques in protic solvents, and none have been made *via* high temperature/pressure (solvothermal) methods. Most are of small nuclearity, with dimers being particularly prevalent. Larger species tend to be heterometallic, and the majority of these contain s-block metal ions. This perhaps suggests that the increased flexibility in the coordination number and geometry of the s-block metal ions allows them to be more easily accommodated into the framework of the cluster, whose (often asymmetric) topology is dictated by the conformation of the calix[8]arene. There are no examples of heterometallic V-3d, V-4f or V-5f clusters. Clearly there remains a vast amount of chemistry to be explored before the coordination chemistry of vanadium is fully mapped out. There does not appear to be a common/dominant structural theme arising from the metallic skeletons of the V clusters thus far, albeit $\{V_2\}$ dimers, $\{V_4\}$ butterflies and $\{V_4\}$ tetrahedra are the most common. The calix[8]arene ligands in these clusters show a variety of conformations and are either fully deprotonated, TBC[8], or singly/doubly deprotonated H_1TBC[8]/H_2TBC[8], as one might expect given the coordination chemistry is primarily established for the V^V ion. The most common coordination motif of the ligand is as an η^2-chelate with two neighbouring O(Ph) atoms bonded to the same V centre.

Co-based clusters

The second biggest family of TBC[8]-supported clusters belongs to homo- and heterometallic complexes of Co^{II}.[14–19] The first, and only homometallic cluster in the family is the aesthetically pleasing $[HNEt_3]_2[Co^{II}_2(H_5TBC[8])_2]$ (**14**) dimer made in 2007 (Fig. 6).[14] Complex **14** was synthesised *via* the solvothermal reaction of $Co(OAc)_2{\cdot}4H_2O$ with H_8TBC[8] and NEt_3 in MeOH at $T = 166$ °C for 72 hours. The centrosymmetric anionic cluster of **14** possesses a metal–oxygen (magnetic) core describing a $[Co_2(OR)_2(HOR)_2]$ dimer in which the Co ions are 'linked' by two Co–O–H···O–Co H-bonds. The Co ions are four coordinate and in distorted tetrahedral $\{CoO_4\}$ geometries, the remaining two O atoms being terminally bonded (deprotonated) O(Ph) atoms of different H_5TBC[8] ligands. The other four O(Ph) atoms on the H_5TBC[8] ligands remain protonated and non-bonded, with both ligands adopting the pleated-loop conformation. Charge balance is provided by two $[Et_3NH]^+$ cations. Magnetic susceptibility measurements revealed the presence of weak antiferromagnetic exchange through the Co–O–H···O–Co H-bonds, with theoretical calculations indicating significant zero-field splitting at the distorted tetrahedral Co sites.[14]

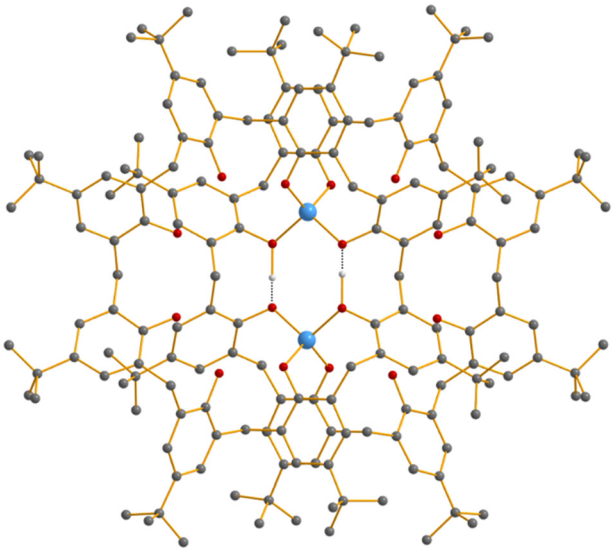

Fig. 6 The structure of the anion of compound **14**. Colour code: Co = sky blue, O = red, C = grey. H = white. The Co–O–H···O–Co H-bonds are shown by the dashed black lines. These H atoms are included, while all others are omitted for clarity.

The remaining Co-based clusters are all heterometallic. The first is a small family of 3d–4f clusters published in 2012 of formula $[Ln^{III}_6Co^{II}_8(TBC[8])_2O_2(OH)_4(CO_3)_2(OAc)_4(HCOO)_2(dmf)_m(H_2O)_n]$ (Ln = Sm (**15a**), $m = 8$, $n = 6$; Ln = Gd (**15b**), Dy (**15c**), $m = 10$, $n = 4$).[15] The complexes were synthesised from the solvothermal reaction of $Ln(OAc)_3{\cdot}6H_2O$, $Co(OAc)_2{\cdot}4H_2O$ and H_8TBC[8] in a basic dmf/MeOH solution (dmf = *N*,*N*-dimethylformamide). The CO_3^{2-} originates from the fixation of atmospheric CO_2 and the formate from the oxidation of MeOH. The structure of **15** (Fig. 7) is rather unusual. Each half of the molecule consists of a central $[Co_2Ln_2(\mu_4\text{-O})]$ square. On one side of this square lies a $[CoLn_2(\mu_3\text{-OH})]$ triangle which shares a vertex at the Ln site. On the other side of the square lies a $[Co_2Ln(\mu_3\text{-OH})]$ triangle which shares the Co–Ln edge of the square. Both triangles are positioned approximately perpendicular to the square. The two remaining Ln ions link the two halves of the molecule together. Each half of the molecule contains one fully deprotonated TBC[8] ligand in the double-cone conformation, with each O(Ph) atom μ-bridging between neighbouring metal ions. Six of these link Co–Ln ions within each half of the cluster, while two bridge the two Ln ions in the central square to the two Ln ions that join the halves together. The Co^{II} ions are of three types, two are six-coordinate and in distorted octahedral $\{CoO_6\}$ geometries, four are five-coordinate and in distorted trigonal bipyramidal $\{CoO_5\}$ geometries, and two are four coordinate and in distorted tetrahedral $\{CoO_4\}$ geometries. The Ln^{III} ions are in two geometries, four being eight coordinate and in square antiprismatic $\{LnO_8\}$ geometries, and two being seven coordinate and in capped trigonal prismatic $\{LnO_7\}$ geometries. Magnetic studies of all three complexes showed the presence of

 This journal is © The Royal Society of Chemistry 2025

Open Access Article. Published on 22 2024. Downloaded on 31.05.2026 00:39:47.
This article is licensed under a Creative Commons Attribution-NonCommercial 3.0 Unported Licence.

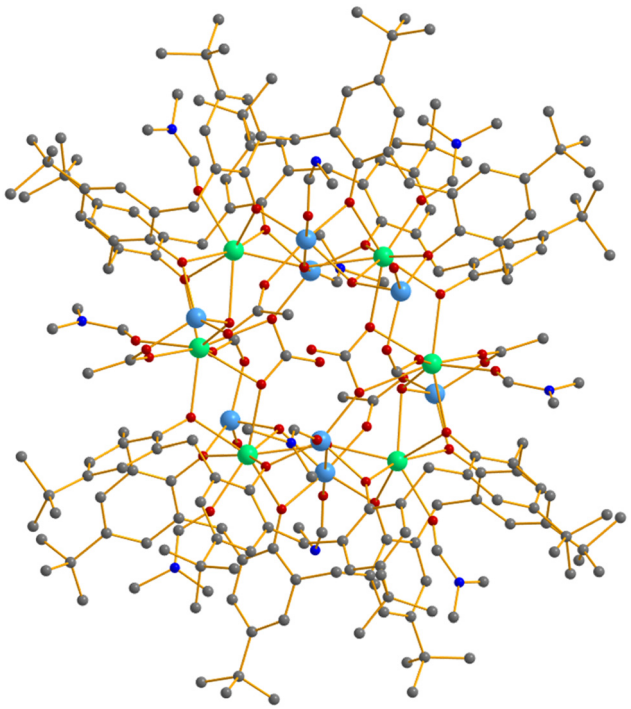

Fig. 7 The structure of compound **15**. Colour code: Co = sky blue, Ln = light green, O = red, N = blue, C = grey. H atoms omitted for clarity.

competing (weak) ferro- and antiferromagnetic exchange interactions.[15]

The isostructural complexes $[Ln^{III}_4Co^{II}_4(TBC[8])_2O_2(def)_x(H_2O)_y]$ (Ln = Dy (**16a**, x = 8, y = 4); Er (**16b**), x = 8, y = 4; Y (**16c**), x = 6, y = 6; Fig. 8) were published in 2017.[16] They were synthesised from the solvothermal reaction of $H_8TBC[8]$, $Co(OAc)_2{\cdot}4H_2O$ and $Ln(OAc)_3{\cdot}6H_2O$ in a basic MeOH/def solution (def = *N*,*N*-diethylformamide) at T = 130 °C for 3 days. The metallic skeleton of **16** describes a $\{Ln^{III}_4Co^{II}_4\}$ square antiprism, with the top and bottom faces being $\{Ln^{III}_2Co^{II}_2\}$ squares with the 3d and 4f metal ions alternating around the square. These are connected by a central, planar μ_4-O^{2-} ion. The upper and lower square faces are connected to each other through the presence of four μ_3-H_2O molecules. The inorganic core is sandwiched between two tail-to-tail, fully deprotonated TBC[8] ligands which adopt the double-cone conformation. In each case four of the O(Ph) atoms are μ-bridging between Co–Ln ions while the remaining four are monodentate, neighbouring pairs chelating to a single Ln ion. The coordination sphere of each metal ion is completed by a solvent molecule. The Ln^{III} ions have two different geometries, two being eight-coordinate and square antiprismatic $\{LnO_8\}$, and two being seven-coordinate with capped octahedral $\{LnO_7\}$ geometry. Likewise, the Co^{II} ions possess two different geometries, five coordinate distorted trigonal bipyramidal $\{CoO_5\}$, and six coordinate distorted octahedral $\{CoO_6\}$. Magnetic studies reveal that the Dy analogue (**16a**) is a single-molecule magnet (SMM), possessing frequency and temperature dependent out-of-phase (χ'') signals in ac susceptibility studies.[16] The ac susceptibility data were fitted to a model assuming a Raman/Orbach relaxation

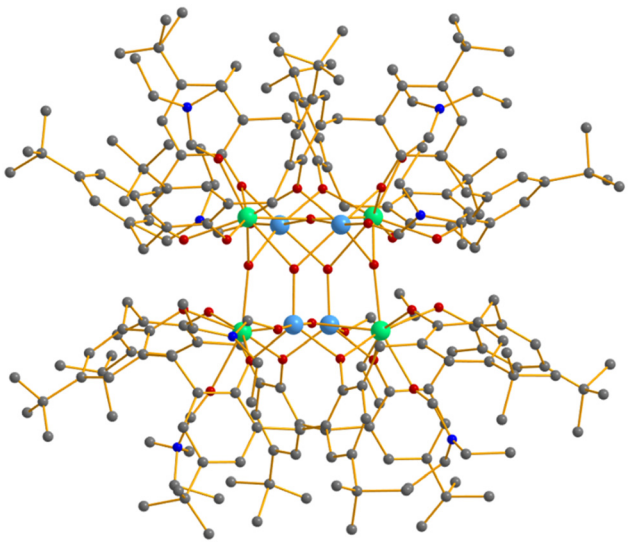

Fig. 8 The structure of compound **16**. Colour code: Co = sky blue, Ln = light green, O = red, N = blue, C = grey. H atoms omitted for clarity.

mechanism of the form $\ln \tau = -\ln[CT^n + \tau_0^{-1}\exp(-U_{eff}/k_BT)]$ to afford U_{eff}/k_B = 10.38 K, $\tau_0 = 9.8 \times 10^{-6}$ s, C = 1500 s^{-1} $K^{-0.4}$, n = 0.4.

In 2020 a family of complexes of formula $[HNEt_3][Ln^{III}_6Co^{II}_6(H_1TBC[8])_3(OMe)_6(OAc)_2(CO_3)(dmf)_6(MeOH)]$ (**17a**, Ln = Y; **17b**, Ln = Eu; **17c**, Ln = Dy; Fig. 9) was published. Each member was synthesised *via* the solvothermal reaction of $Co(OAc)_2{\cdot}4H_2O$, $Ln(OAc)_3{\cdot}6H_2O$ and $H_8TBC[8]$ in a basic MeOH/dmf solution at T = 150 °C for 3 days.[17] At the centre of the cluster lies a μ_6-CO_3^{2-} anion, generated *in situ* from the fixation of atmospheric CO_2, which templates the formation of a $\{Co_6\}$

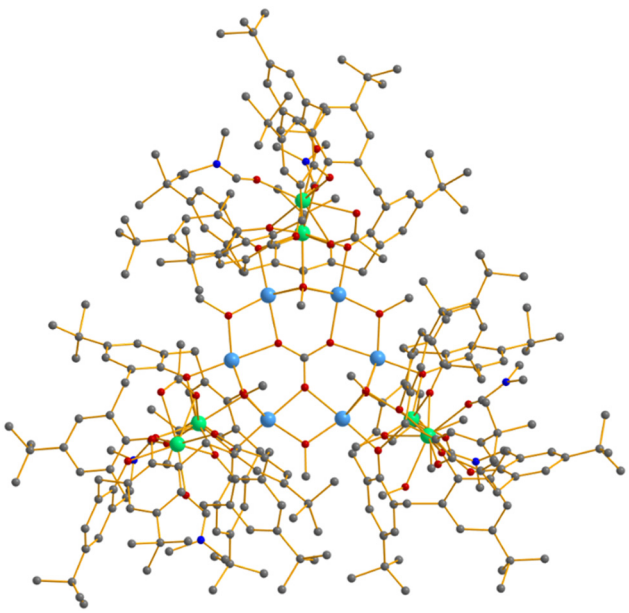

Fig. 9 The structure of the anion of compound **17**. Colour code: Co = sky blue, Ln = light green, O = red, N = blue, C = grey. H atoms omitted for clarity.

Open Access Article. Published on 22 2024. Downloaded on 31.05.2026 00:39:47.
This article is licensed under a Creative Commons Attribution-NonCommercial 3.0 Unported Licence.

wheel. The outer rim of this wheel is bridged alternately by three μ-OH^- ions and three μ_3-OH^- ions, the latter also bridging to a Ln ion in the {Ln_2TBC[8]} fragments. These are all positioned 'above' the {Co_6} plane forming a bowl-shaped cage. The three, fully deprotonated, TBC[8] ligands adopt the double-cone conformation, each encapsulating a {Ln_2} dimer and using two of their O(Ph) arms to bridge between the two metals, {$Ln_2(OR)_3$}. The third bridging O atom in the dimer is provided by either an acetate or methanol. Two of the O(Ph) arms are used to connect the {Ln_2} dimer to the {Co_6} wheel across the same edge as the μ_3-OH^- ions. The remaining three O(Ph) atoms are monodentate, with one per ligand protonated. The coordination spheres of all the Ln^{III} ions are completed by a molecule of dmf, and result in either seven coordinate {LnO_7} capped octahedra, seven coordinate capped {LnO_7} trigonal prisms or eight coordinate {LnO_8} biaugmented trigonal prisms. Each Co^{II} ion is five coordinate and in a distorted trigonal bipyramidal {CoO_5} coordination geometry. Magnetic studies suggest that the Eu analogue exhibits spin glass behaviour, while the Dy version is an SMM.[17]

The core of the complex $[Co^{II}_2Th^{IV}_4O_2(OH)_2(H_1TBC[8])_2(dmf)_6]$ (**18**) describes two [$CoTh_3O(OH)$] tetrahedra, sharing a {Th_2} edge (Fig. S7, ESI†).[18] The μ_4-O^{2-} ions sit in the centre of each tetrahedra, with the μ-OH^- ions capping one {Th_2} edge each. The hepta-deprotonated H_1TBC[8] ligands adopt the double-cone conformation, with four O(Ph) atoms μ-bridging between neighbouring Co–Th (×3), Th–Th (×1) metal ions across edges of the {$CoTh_3$} tetrahedra. The remaining four O(Ph) atoms are all terminally bonded to Th ions. The latter are eight coordinate and in distorted square antiprismatic {ThO_8} geometries, while the two Co ions are both 5-coordinate {CoO_5} and trigonal bipyramidal. The six dmf molecules sit in the hydrophobic calix[8]arene cavities, one terminally bonded to each of the Co and Th ions.

The most recent examples of TBC[8]-supported Co clusters are a family of heterometallic Co–Li/Na species reported in 2022.[19] The complex $[Co^{II}_2Li_8(OH)_2(TBC[8])Br_2(MeCN)_4(THF)_6]$ (**19**) was made from the reaction of $CoBr_2$, H_8TBC[8], and LiO^tBu in THF (Fig. S8, ESI†). The metallic skeleton of **19** describes three edge sharing $[Co_xLi_{4-x}]$ squares, connected to one additional Li ion at each end. This gives it a ladder- or rod-like appearance. In the centre lies a $[Co_2Li_2]$ square, two edges being singly bridged by a μ-O(Ph) atom from the TBC[8] ligand, with the other two edges being doubly bridged by two μ_4-OH^- and two μ-Br^- ions. The μ_4-OH^- ions further bridge to two Li ions on each side of the square, thus forming $[CoLi_3]$ squares on each side of the central square. The three remaining edges of these squares are singly bridged by a $\mu_{2/3}$-O(Ph) atom from the TBC[8] ligand. The μ_3-O(Ph) atom further bridges to a single Li ion at each end of the cluster, forming a $[Li_3O]$ triangle. All ten metal ions are four coordinate and in distorted tetrahedral geometries. The coordination spheres of the Li ions are completed by a combination of THF and MeCN molecules. The TBC[8] ligand is fully deprotonated and adopts the pleated-loop conformation, with six/two O(Ph) atoms being $\mu_{2/3}$-bridging, respectively.

The related complex $[Co^{II}_2Li_6(OH)_2(TBC[8])Br_2(MeCN)_4]$ (**20**) can be obtained from the reaction of $CoBr_2$, LiO^tBu and H_8TBC[8] in Et_2O.[19] The structure of **20** (Fig. S9, ESI†) is very similar to **18** but with the peripheral Li ions and terminal THF molecules being absent. Variations in reaction stoichiometry and reagents appear to play an interesting role in product identity for both **19** and **20**, particularly with regard to the Co:Li ratio/positional disorder at the metal sites, such that several non-stoichiometric analogues have been isolated.[19]

The sole Na analogue in the family is the complex $[Co^{II}_4Na(H_4TBC[8])_2Br(MeCN)_6]$ (**21**) made from the reaction of $CoBr_2$, H_8TBC[8] and NaH in THF.[19] The structure of **21** (Fig. S10, ESI†) is highly unusual. The metallic skeleton is an irregular polyhedron, perhaps best described as a highly distorted {Co_4Na} square based pyramid, with a Co^{II} ion at the apex and three Co^{II} ions and one Na ion forming the square base. However, not all of these ions are directly connected to each other. The apical Co^{II} ion is linked to one Co^{II} ion in the square base through a μ-bridging Br^- ion and one μ-O(Ph) atom. In turn, this Co^{II} ion is bridged to the other Co^{II} ions in the square base *via* two μ-O(Ph) atoms from the same H_4TBC[8] ligand. The remaining five O(Ph) atoms are uncoordinated, sharing four H-bonds, with the ligand adopting a pseudo-chair loop conformation. The second calix[8]arene ligand is also quadruply deprotonated, H_4TBC[8], but does not bridge between any metal centres. Instead, it adopts the pleated-loop conformation in which each neighbouring pair of O(Ph) atoms chelate to a single metal centre. A total of four H-bonds are observed between the O(Ph) atoms. The four Co^{II} ions are of three types. Two are four coordinate and in distorted tetrahedral {CoO_3N} geometries, the fourth site being occupied by a MeCN molecule. There is an additional long contact to the μ-Br^- ion (~3 Å). One Co ion is five coordinate and in a distorted trigonal planar {CoO_3NBr} geometry, again coordinating a MeCN molecule. The fourth Co ion is six coordinate and in a distorted octahedral {CoO_3N_2Br} geometry, with its coordination sphere completed by two MeCN molecules. The Na ion is four coordinate and in a distorted {NaO_2BrN} coordination geometry, with another MeCN molecule completing its coordination sphere.

Summary of Co-based clusters

The coordination chemistry of cobalt is (thus far) dominated by the Co^{II} ion, albeit with just one homometallic cluster, a dimer. All other reported compounds are heterometallic, being either Co-f block or Co-s block species. The prevalence of heterometallic over homometallic compounds is reflective of that seen for vanadium above, and remains a common theme in what follows below. The metallic skeletons of Co-based compounds are often based on dimers and tetramers. The latter can be squares, butterflies or tetrahedra, with larger species also being based on these units, *e.g.* square-based pyramids and square antiprisms. The calix[8]arene ligands in these clusters display a variety of conformations and protonation levels from the doubly deprotonated H_6TBC[8] to the fully deprotonated TBC[8], with the O(Ph) atoms bonding in both terminal (with

 This journal is © The Royal Society of Chemistry 2025

Open Access Article. Published on 22 2024. Downloaded on 31.05.2026 00:39:47. This article is licensed under a Creative Commons Attribution-NonCommercial 3.0 Unported Licence.

neighbouring atoms chelating the same metal centre) and μ-bridging modes.

Fe-based clusters

All three Fe-based clusters in the CSD were published between 2007–2010 and are heterometallic, two include Ge and one includes K.[20–22] $[Ge^{II}_4(TBC[8])][Fe^0_2(CO)_8]$ (**22**; Fig. S11, ESI†) was synthesised from the reaction of $[Ge_4(TBC[8])]$ with $[Fe_2(CO)_9]$ in benzene.[20] Complex **22** largely retains the same overall structural features of the $[Ge^{II}_4TBC[8]]$ starting material, in which two $\{Ge_2O(Ph)_2\}$ rhombs occupy two separate halves of the molecule, related by a C_2 axis. The two $\{Fe(CO)_4\}$ groups are bonded to the two Ge ions that are positioned outwith the central cavity of the TBC[8] ligand, pointing downwards with respect to the top of the ligand bowl. The TBC[8] ligand adopts a distorted saddle conformation, wrapping around the Ge ions such that four O(Ph) atoms are bonded to each $\{Ge_2\}$ pair; two terminally bonded and two μ-bridging. The Fe atoms are formally zero valent, with all four Ge ions in the +2 oxidation state. Interestingly, the same reaction but using the *para*-unsubstituted $H_8C[8]$ ligand results in the formation of $[Ge^{IV}_4(C[8])][Fe^{-I}_2(CO)_8]_4$ (**23**) (Fig. 10).[21] In this case the reaction proceeds *via* (an unexpected) reductive decarbonylation, with extrusion of one bridging CO group in $[Fe_2(CO)_9]$ and the formation of four $[GeFe_2]$ three-membered rings, arranged in a tetrahedral fashion around the C[8] ligand. Formally, the reaction involves oxidation of Ge^{II} to Ge^{IV} and reduction of the diiron fragments to $[Fe_2(CO)_8]^{2-}$.

The final Fe-based cluster in the database is the complex $[Fe^{II}_4K_4O_2(H_2O)_2(H_2TBC[8])_2(MeCN)_6]$ (**24**; Fig. S12, ESI†) which results from the reaction of $[K_2Fe_2(O^tBu)_6(THF)_2]$ with $H_8TBC[8]$ in toluene, followed by crystallisation from MeCN.[22] The ASU in **24** contains a near-linear Fe–O–Fe dimer in which the μ_4-O^{2-} ion further bridges to two K ions lying in a perpendicular plane. Both Fe ions are four coordinate and in distorted tetrahedral $\{FeO_4\}$ geometries, the other three O-atoms deriving from the $H_2TBC[8]$ ligand. Symmetry expansion reveals that the four K ions form a central square rhomb, connected by four and two bridging MeCN and H_2O molecules, respectively. The hexa-deprotonated $H_2TBC[8]$ ligands adopt the double-cone conformation, and present an unusual bonding motif. Four O(Ph) atoms are μ-bridging between the Fe and K ions, two are terminally bonded to Fe ions, and the two protonated O-atoms are non-bonded. In the latter case, the associated Ph group bonds side-on (η^6) to a K ion.

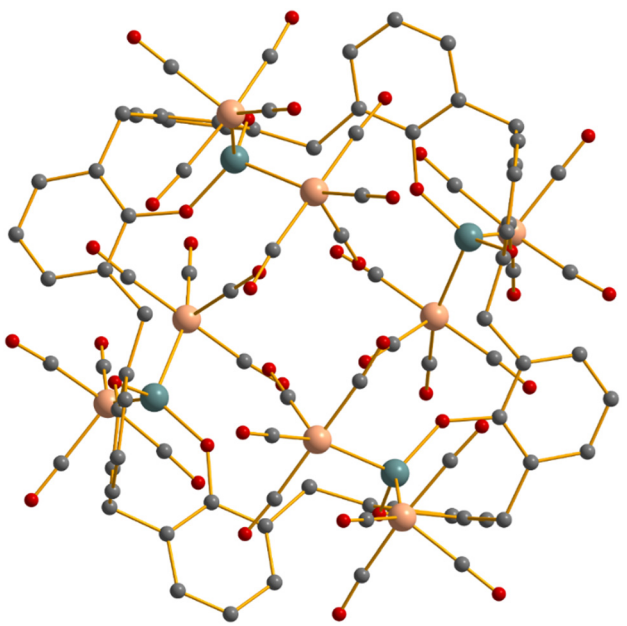

Fig. 10 The structure of compound **23**. Colour code: Fe = pale orange, Ge = teal, O = red, C = grey. H atoms omitted for clarity.

Summary of Fe-based clusters

Here it is very clear that the coordination chemistry of $H_8TBC[8]$ with Fe is almost completely unknown, with only three heterometallic complexes published, two rooted in Fe carbonyl chemistry, with the other being an Fe-s block complex. There are zero examples of homometallic Fe clusters in any oxidation state and no clusters containing more than four Fe centres. The calix[8]arene ligands are present in either their fully deprotonated, TBC[8]/C[8], or doubly protonated, $H_2TBC[8]$, forms in distorted saddle and double-cone conformations, respectively. The O(Ph) atoms of the ligands adopt two bonding motifs – terminal, with neighbouring atoms chelating the same metal centre, and μ-bridging. In each case the latter directs the formation of $\{Fe_2\}$ dimers.

Mn-based clusters

There are also only three Mn-based clusters in the CSD, all published between 2011–2013.[23–25] The first of these was the complex $[Mn^{III}_2Na_4(H_5TBC[8])_2(CO_3)_2(dmf)_6]$ (**25**; Fig. 11) which was made from the reaction of $MnCl_2{\cdot}4H_2O$, $H_8TBC[8]$ and NaO_2CCMe_3 in a basic MeOH/dmf solution.[23] The pivalate anion is not incorporated into the structure but its presence appears vital for cluster formation. We note with interest that the well-known complex $[Mn_6O_2(O_2CR)_{10}(solvent)_4]$ (R = CMe_3, Ph) is often a major/minor product in Mn-$H_8TBC[8]$ reactions with certain carboxylates.[23] The metallic skeleton of **25** contains a central $\{Na_4\}$ square, flanked on both sides by a Mn^{III} ion. The metals are linked together by two μ_5-CO_3^{2-} ions, formed from the fixation of atmospheric CO_2, which each bridge to all four Na ions and one Mn^{III} ion on the same face of the square. The remaining bridging in the $\{Mn_2Na_4\}$ moiety comes from two μ_3-bridging and two μ-bridging dmf molecules. The former sit above/below the $\{MnNa_2\}$ triangles in the two halves of the molecule. The latter bridge between two Na ions across an edge of the $\{Na_4\}$ square. The presence of multiple bridging dmf molecules, and in two different coordination modes, is rather unusual. The calix[8]arene ligands adopt the pleated-loop conformation, sandwiching the inorganic core. They are triply deprotonated with six of the eight O(Ph) atoms being monodentate and each neighbouring pair chelating to a metal centre in the $\{MnNa_2\}$ triangle. The remaining two (neighbouring) HO(Ph) arms are uncoordinated. The six

Open Access Article. Published on 22 2024. Downloaded on 31.05.2026 00:39:47.
This article is licensed under a Creative Commons Attribution-NonCommercial 3.0 Unported Licence.

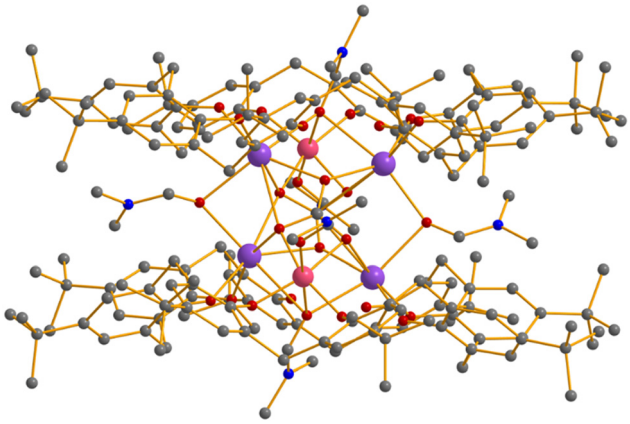

Fig. 11 The structure of compound **25**. Colour code: Mn^{III} = magenta, Na = purple, O = red, N = blue, C = grey. H atoms omitted for clarity.

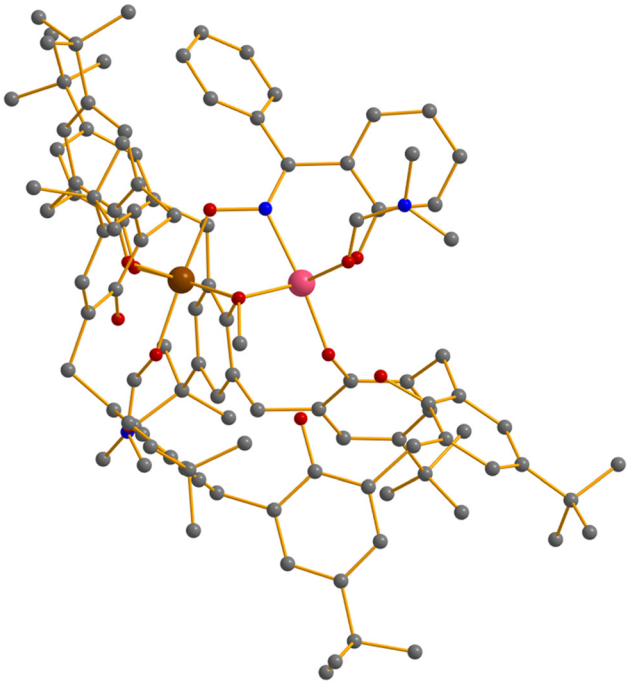

Fig. 12 The structure of compound **26**. Colour code: Mn^{III} = magenta, Mn^{IV} = brown, O = red, N = blue, C = grey. H atoms omitted for clarity.

coordinate Mn^{III} ions have their coordination spheres completed with two (*trans*) dmf ligands and are in Jahn–Teller (JT) distorted octahedral $\{MnO_6\}$ geometries, the JT axis being defined by the O(dmf)–Mn–O(dmf) vector. Examination of the extended structure of **25** reveals the formation of large and aesthetically pleasing infinite stacked tubular assemblies, and that packing of neighbouring tubules results in the formation of solvent-filled channels within the structure.[23] The structure of **25** has some striking similarities to **24** (Fig. S12, ESI†) despite the different d- and s-block metals employed and the entirely different synthetic methodologies, highlighting perhaps the dominant structure directing role of calix[8]arene ligands. The presence of the bridging dmf molecules is similar to that seen in the vanadium chemistry described above.

The second Mn-based cluster published employed a heteroleptic ligand strategy which exploited the complementary ligand bridging modes of H_8TBC[8] and phenyl salicylaldoxime (Ph-saoH_2) to drive the formation of a heterovalent $\{Mn^{III}Mn^{IV}\}$ dimer.[24] Thus, the reaction of $Mn(NO_3)_2{\cdot}4H_2O$, H_8TBC[8] and Ph-saoH_2 in a basic dmf/MeOH solution afforded $[Mn^{III}Mn^{IV}(H_4TBC[8])(Ph\text{-}sao)(\mu\text{-}OMe)(dmf)_2]$ (**26**; Fig. 12). The magnetic core of **26** is a $[Mn^{III}O(Me)O(Ph)(NO)Mn^{IV}]$ moiety in which the two Mn ions are triply bridged by a single μ-OMe ion, a single μ-O(Ph) atom from the calix[8]arene, and the –N–O– oxime unit of Ph-sao^{2-}. The Mn^{III} ion has its coordination sphere completed by the terminally bonded alkoxide O-atom of Ph-sao^{2-} and a molecule of dmf, with the O(dmf)–Mn–O(Ph) vector defining the JT axis. There is also a single dmf coordinated to the Mn^{IV} ion. Both Mn ions are six coordinate and in distorted octahedral geometries. The quadruply-deprotonated H_4TBC[8] ligand adopts a conformation that is best described as being somewhere between a double-cone and a pleated-loop, wherein three phenol moieties adopt a cone orientation and the other five resemble a regular pleated-loop. The four deprotonated O(Ph) atoms adopt different coordination modes, three being monodentate and the fourth μ-bridging. The four protonated HO(Ph) arms are non-coordinated. It would appear therefore that the presence of the bulky phenolic oxime prevents full adoption of either of the more common calix[8]arene conformations, and restricts the nuclearity of the complex formed.

Magnetic susceptibility and magnetisation studies on **26** revealed the presence of a moderate ferromagnetic interaction between the two metal ions (J = +9.81 cm^{-1}, g = 1.99; $\hat{H} = \mu_B B\sum_i g_i\hat{S}_i - 2\sum_{i<j} J_{i,j}\hat{S}_i\cdot\hat{S}_j + \sum_i D_i\left(\hat{S}_z^2 - S(S+1)/3\right)$ formalism) resulting in the stabilisation of an S = 7/2 ground state. A fit of the magnetisation data in the context of the giant spin model suggested the ground state to have a significant zero-field splitting, $D_{S=7/2}$ = −0.91 cm^{-1}, with ac susceptibility data confirming slow relaxation of the magnetisation through the presence of temperature and frequency dependent out-of-phase (χ'') signals below $T \approx 4$ K. Complex **26** was therefore the first reported TBC[8]-based SMM.

The complex $[Mn^{II}_5(H_4TBC[8])(OH)_2(OMe)_{1.5}(HCOO)(OAc)_{0.5}(O_2CNMe_2)(dmf)_5]$ (**27**; Fig. 13) was synthesised *via* the solvothermal (T = 130 °C, 3 days) reaction of $Mn(OAc)_2{\cdot}4H_2O$, H_8TBC[8] and KCl in a basic MeOH/dmf solution.[25] Neither K^+ or Cl^- are incorporated into the structure of the product, but it would appear that addition of the salt is required for **27** to form. The dimethylcarbamate and formate anions are generated *in situ* from the decomposition of dmf/oxidation of MeOH, respectively. The metallic skeleton of **27** describes a $\{Mn_5\}$ square based prism, with the apex connected to the square base *via* a combination of μ_3-OMe and μ_3-OH ions. The four Mn ions in the base are further connected by the μ_3-O_2CNMe_2 ligand that sits below the square. All five Mn^{II} ions are six coordinate and in distorted octahedral $\{MnO_6\}$ geometries.

This journal is © The Royal Society of Chemistry 2025

Open Access Article. Published on 22 2024. Downloaded on 31.05.2026 00:39:47.
This article is licensed under a Creative Commons Attribution-NonCommercial 3.0 Unported Licence.

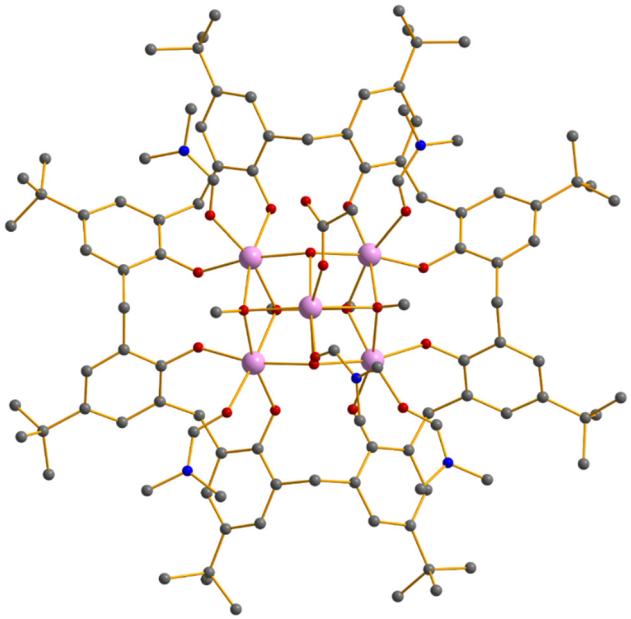

Fig. 13 The structure of compound **27**. Colour code: Mn^{II} = pale pink, O = red, N = blue, C = grey. H atoms omitted for clarity.

Each has a single terminally coordinated dmf molecule directed above the square, with the apical Mn ion bonded to an additional carboxylate (OAc/O_2CH) ligand. The calix[8]arene is tetra-deprotonated, $H_4TBC[8]$ and sits below the $\{Mn_4\}$ square in the pleated-loop conformation, each neighbouring pair of O(Ph) atoms chelating to a single Mn^{II} ion. Magnetic susceptibility studies revealed the presence of weak antiferromagnetic exchange (J = −2 to 3 cm^{-1}) between neighbouring Mn^{II} ions.[25]

Summary of Mn-based clusters

Given that the coordination chemistry of $H_4TBC[4]$ with Mn is very well established, and shown to be a hugely fruitful source of numerous polymetallic clusters,[1,26] the isolation of only three Mn-based complexes of $H_8TBC[8]$ is surprising, in turn suggesting that a systematic investigation of this chemistry has not been performed. Drawing conclusions regarding structural trends is rather difficult, though two of the three metallic skeletons are based on squares. It is interesting to see that all three common Mn oxidations states (Mn^{II}, Mn^{III} and Mn^{IV}) exist in the three complexes isolated, and all the calix[8]arenes are only partially deprotonated, $H_4TBC[8]$ or $H_5TBC[8]$. We also note that in two of the three complexes isolated, molecules not added to the reaction mixtures become incorporated into the structures – CO_3^{2-} from the fixation of CO_2, formate from the oxidation of MeOH and dimethylcarbamate from the breakdown of dmf. This perhaps suggests that the deliberate introduction of these (or similar) molecules would be worth exploring. Indeed, the presence of the CO_3^{2-} ion is a common theme in the Ln^{III}-based chemistry discussed below (and in Ln coordination chemistry more generally), but it is very rarely/intentionally employed as a bridging ligand.

Ni-based clusters

The sole Ni-based cluster in the CSD is the complex $[Ni^{II}_2Th^{IV}_5O_4(OH)_2(H_1TBC[8])_2(dmf)_5(MeOH)_2]$ (**28**; Fig. 14).[18] The metallic skeleton of **28** describes a highly distorted $\{Ni_2Th_4\}$ octahedron, capped on one face by the fifth Th^{IV} ion, and stabilised by the presence of four O^{2-} ions which sit on the four equatorial edges of the $\{Ni_2Th_2\}$ square. Three are μ_4-bridging (2 × $\{Th_3Ni\}$, 1 × $\{Th_2Ni_2\}$), and one is μ_3-bridging (1 × $\{Th_3\}$). The two Th^{IV} apices are connected to this square by eight {OR} alkoxides, one on each edge. Six are derived from μ-O(Ph) atoms of the calix[8]arene ligands, with the remaining two, on neighbouring edges, being μ_3-OH ions. The latter further bridge to the remaining Th^{IV} ion, which caps a $\{Ni_2Th\}$ face of the octahedron. The hepta-deprotonated $H_1TBC[8]$ ligands lie approximately perpendicular to each other, sandwiching the metal–oxygen core, and adopt the double-cone conformation. Six of the eight O(Ph) atoms are μ-bridging and two (neighbouring) O-atoms are monodentate. A solvent molecule completes the coordination at each metal centre, a dmf on the eight coordinate Th ions and a MeOH on the six coordinate Ni ions.

Summary of Ni-based clusters

The lack of any homometallic (or 3d–4f) Ni clusters is surprising, particularly due their potentially appealing magnetic properties. Perhaps it is even more surprising that there are no homometallic/heterometallic clusters of Ni with $H_4TBC[4]$, both highlighting glaring omissions in the literature. A systematic exploration of Ni-based clusters with both $H_4TBC[4]$ and $H_8TBC[8]$ is required across a range of experimental

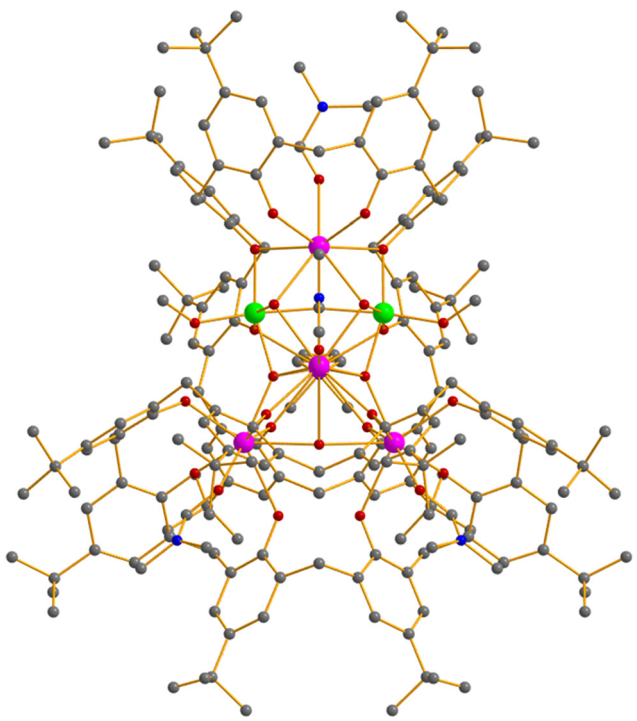

Fig. 14 The structure of compound **28**. Colour code: Ni = green, Th = deep pink, O = red, N = blue, C = grey. H atoms omitted for clarity.

Open Access Article. Published on 22 2024. Downloaded on 31.05.2026 00:39:47. This article is licensed under a Creative Commons Attribution-NonCommercial 3.0 Unported Licence.

conditions to map out the associated coordination chemistry of these systems.

Cr-based clusters

There is a single family of isostructural Cr-based clusters of formula $[Cr^{III}Ln^{III}_6O_2(OH)(TBC[8])_2(H_2O)_4(dmf)_5(MeOH)_2]$ (Ln = Gd (**29a**), Tb (**29b**), Dy (**29c**), Tm (**29d**); Fig. 15),[27] the general metallic skeleton of which describes a capped distorted octahedron. The $\{Ln_5Cr\}$ octahedron is bridged internally *via* two μ_4-O^{2-} ions; an alternative description of the core is therefore of two edge-sharing $\{Ln_4O\}/\{Ln_3CrO\}$ tetrahedra. The remaining Ln ion caps a $\{Ln_2Cr\}$ face, being coordinated to it through the presence of three μ_3-bridging O-atoms derived from H_2O molecules. The sole μ-bridging OH^- ion spans a $\{Ln_2\}$ edge of the octahedron. Both fully deprotonated TBC[8] ligands adopt the double-cone conformation sandwiching the inorganic core of the molecule, lying perpendicular with respect to each other. They coordinate in two different ways. The first uses six of its O(Ph) atoms to μ-bridge between neighbouring metal ions, the two remaining O(Ph) atoms, positioned next to each other, being monodentate and chelating a single Ln ion.

The second TBC[8] ligand contains five monodentate O(Ph) atoms, all positioned next to each other, and three μ-bridging O(Ph) atoms. The Cr^{III} ion is six coordinate and in a distorted $\{CrO_6\}$ octahedral geometry, the sixth site being occupied by a MeOH molecule. The Ln^{III} ions are of two types: five are eight coordinate and in square antiprismatic $\{LnO_8\}$ geometries, and one is seven coordinate and in pentagonal bipyramidal $\{LnO_7\}$ geometry, their coordination completed through the presence of dmf, MeOH and water molecules. Magnetic measurements revealed the Tb^{III} analogue (**29b**) to be a SMM. A fit of the ac susceptibility data to the Arrhenius law ($\tau = \tau_0 \exp[U_{eff}/(k_BT)]$) revealed an effective energy barrier to magnetisation reversal of U_{eff}/k_B = 18.13 K with a pre-exponential factor of $\tau_0 = 7.5 \times 10^{-8}$ s.[27]

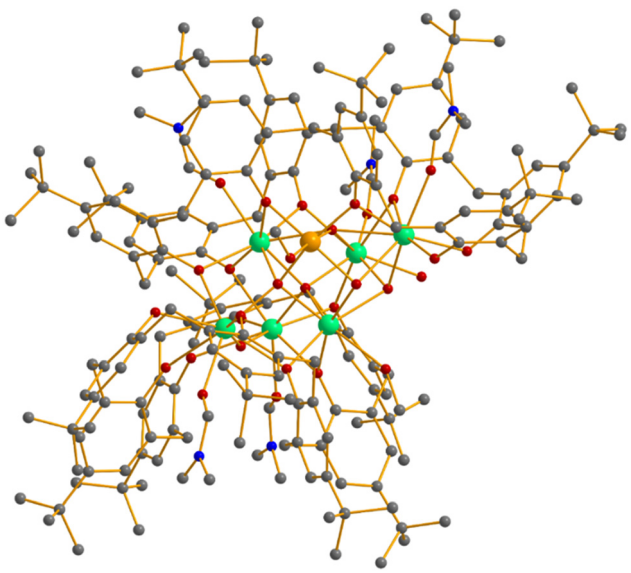

Fig. 15 The structure of compound **29**. Colour code: Cr = golden, Ln = light green, O = red, N = blue, C = grey. H atoms omitted for clarity.

Summary of Cr-based clusters

As with the limited coordination chemistry of Ni^{II}, $Fe^{II/III}$, Co^{II}, $Mn^{II/III/IV}$ and Co^{II} described above, the lack of any published homometallic Cr^{III} compounds of H_8TBC[8] (and H_4TBC[4]) reveals a serious gap in knowledge when it comes to polymetallic clusters of paramagnetic 3d ions. The isolation of **29** clearly shows this (and more 3d–4f chemistry) will be possible, and that it will lead to some exciting new compounds. We also note also that there are zero H_8TBC[8]-supported clusters of Cu. All of this chemistry remains to be explored, but is clearly rife for exploitation.

Ln-based clusters

The first Ln-based cluster published was $[Eu^{III}_2(H_2TBC[8])(dmf)_5]$ (**30**) reported in 1987, made from the reaction of $Eu(ClO_4)_3$ and H_8TBC[8] in a basic dmf solution (Fig. S13, ESI†).[28] The two Eu^{III} ions are bridged by two μ-O(Ph) atoms from the H_2TBC[8] ligand and one μ-O(dmf) atom, affording a $\{Eu_2(OR)_3\}$ core. The remaining six O(Ph) atoms on the calix[8]arene are monodentate, with two being protonated as evidenced by the significantly larger Eu–O bond lengths. The ligand adopts a double-cone conformation with near-twofold rotational symmetry. The Eu^{III} ions are both eight coordinate and in $\{EuO_8\}$ bicapped trigonal prismatic geometries. The dimeric $\{Ln_2\}$ unit is extremely common in the coordination chemistry of TBC[8] with lanthanide ions, and indeed there are multiple isostructural $[Ln^{III}_2(H_2TBC[8])(solvent)_5]$ complexes reported which differ only in the coordinated solvent present (Ln = Eu, La, Pr, Lu, Tm; solvent = dmf, dmso; Fig. S14, ESI†).[29–32]

A related monomeric complex, $[Eu^{III}(H_6TBC[8])(NO_3)(dmf)_4]$ (**31**; Fig. S15, ESI†) can be made from the reaction of $Eu(NO_3)_3$, H_8TBC[8] and K_2CO_3 in a basic dmf solution at T = 60 °C.[33] The doubly deprotonated H_6TBC[8] ligand adopts a pleated-loop conformation, bonding to the Eu^{III} ion in a bidentate coordination mode. The metal is eight coordinate and in a distorted $\{EuO_8\}$ square antiprismatic geometry, with the remaining coordination sites being filled with dmf molecules and a bidentate nitrate ion. A similar compound, $[Gd^{III}(H_6TBC[8])Cl(dmso)_4]$ (**32**; Fig. S16, ESI†), can be made *via* the reaction of H_8TBC[8] with $GdCl_3{\cdot}6H_2O$ in a basic MeCN/dmso solution, followed by diffusion with hexane.[34] The structure of **32** is essentially the same as that in **31** but with a single, monodentate Cl^- ion replacing the bidentate NO_3^-. The same paper also reported the synthesis of a number of Ln^{III} complexes varying in nuclearity form Ln_1–Ln_7 from a series of related chemical reactions. Interestingly, in a number of experiments the same general $[Ln^{III}_2(H_2TBC[8])(solvent)_5]$ complex was obtained and the five new complexes discovered all contain a related $\{Ln_2\}$ moiety which is in fact a smaller fragment in the construction of frameworks generally based on octahedra. In each case the calix[8]arene adopts either a

 This journal is © The Royal Society of Chemistry 2025

Open Access Article. Published on 22 2024. Downloaded on 31.05.2026 00:39:47.
This article is licensed under a Creative Commons Attribution-NonCommercial 3.0 Unported Licence.

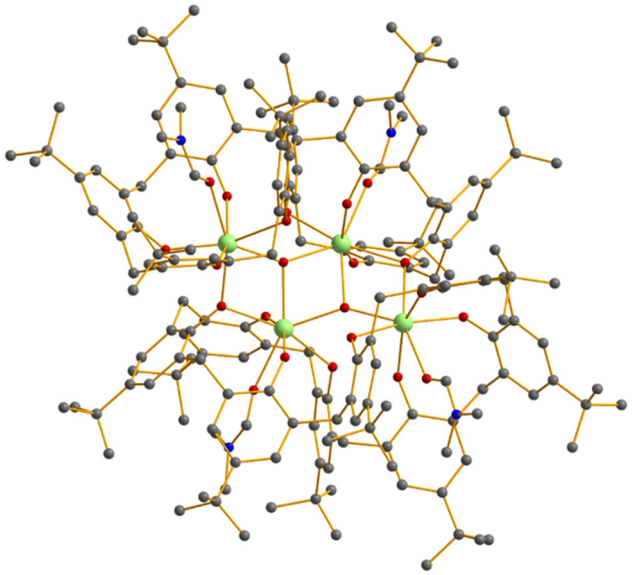

Fig. 16 The structure of compound **33**. Colour code: Ce = lime green, O = red, N = blue, C = grey. H atoms omitted for clarity.

perfect or near-perfect double-cone conformation, but with significant differences in the degree of deprotonation.

Reaction of H_8TBC[8] with $Ce(NO_3)_3{\cdot}6H_2O$ in a basic MeCN/dmf solution, followed by diffusion with hexane, affords the complex $[Ce^{IV}{}_4O_2(H_2TBC[8])_2(dmf)_4]$ (**33**; Fig. 16).[34] At the centre of the molecule lies a non-planar/bowl-shaped $\{Ce_4O_2\}$ butterfly. The Ce^{IV} ions are all seven-coordinate and in distorted $\{CeO_7\}$ pentagonal bipyramidal geometries. Each H_2TBC[8] ligand exists as the hexa-anion, H_2TBC[8], with two intra-molecular H-bonds between neighbouring O(Ph) atoms per calix[8]arene molecule, and bridges three Ce^{IV} ions across one side of the butterfly. Four ligated dmf molecules complete the Ce^{IV} coordination spheres, occupying the cavities generated by each of the H_2TBC[8] molecules.

A similar reaction but employing $TbCl_3{\cdot}6H_2O$ in a basic MeCN/dmso solution affords the complex $[Tb^{III}{}_5O(OH)_4(H_3TBC[8])Cl(dmso)_8(H_2O)_3]Cl_3$ (**34**; Fig. 17).[34] The metallic skeleton of **34** describes a distorted square-based pyramid. The Tb^{III} ions in the square base are connected to each other *via* one μ_4-O^{2-} ion and four μ-O(Ph) atoms, and to the apical Tb^{III} ion through four μ_3-OH^- ions, one on each triangular face of the pyramid. The coordination sites of the metal ions are completed by the presence of several terminally bonded solvent molecules (dmso, H_2O), with the dmso molecules occupying the cavities generated by each of the H_3TBC[8] molecules. The Tb^{III} ions are eight coordinate and in square antiprismatic $\{TbO_8\}$ or $\{TbO_7Cl\}$ geometries. The three protonated arms of the H_3TBC[8] ligand are each H-bonding to one Cl^- counter anion. The latter are also H-bonded to the terminally bonded H_2O molecules. Perhaps surprisingly, the apical Tb^{III} ion is not coordinated to the H_3TBC[8] ligand at all, being connected to the rest of the molecule only through the four μ_3-OH^- ions. Its "exterior" square face is entirely comprised of four terminally ligated solvent molecules (3 × dmso, 1 × H_2O), perhaps suggesting the possibility of further cluster growth by solvent substitution.

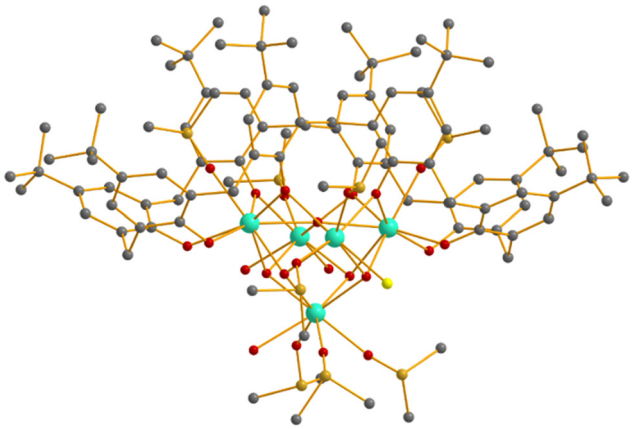

Fig. 17 The structure of the cation of compound **34**. Colour code: Tb = cyan, O = red, C = grey, S = dark yellow, Cl = yellow. H atoms omitted for clarity.

Repeating the reaction that produces **33** but using a different solvent combination (MeOH/dmf) and in the presence of NH_4ClO_4 results in the formation of $[Ce^{IV}{}_6O_4(H_2TBC[8])_2(OMe)_4(dmf)_6]$ (**35**; Fig. 18).[34] The metallic skeleton of **35** is a slightly 'flattened' or 'squashed' $\{Ce_6\}$ octahedron. The two apical sites are connected to the four ions in the square plane (and to each other) *via* two μ_4-O^{2-} ions, four μ-OMe^- ions and four μ-O(Ph) atoms from the H_2TBC[8] ligands. The remaining two, near linear, μ-O^{2-} ions each link neighbouring Ce^{IV} ions across an edge of the square plane. Each H_2TBC[8] exists as a hexa-anion – there is one intra-ligand H-bond between neighbouring O(Ph) atoms per molecule and one inter-ligand H bond – and bridges three Ce^{IV} ions across one triangular face of the octahedron. The dmf molecules again occupy the calixarene

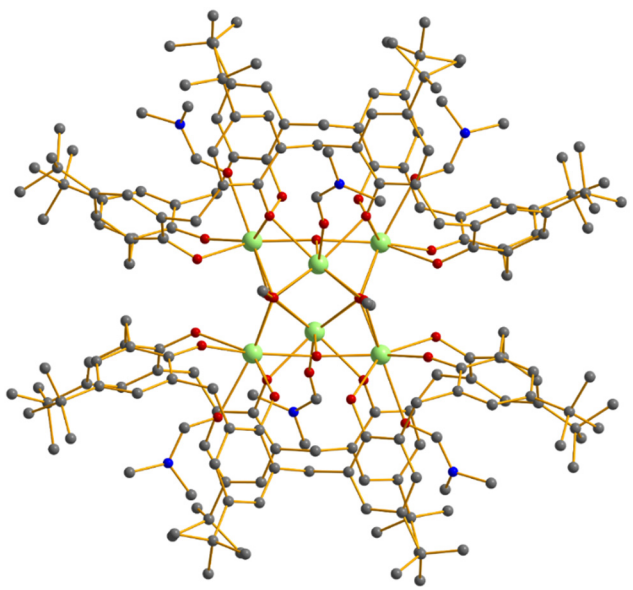

Fig. 18 The structure of compound **35**. Colour code: Ce = lime green, O = red, N = blue, C = grey. H atoms omitted for clarity.

Open Access Article. Published on 22 2024. Downloaded on 31.05.2026 00:39:47.
This article is licensed under a Creative Commons Attribution-NonCommercial 3.0 Unported Licence.

cavities. All six Ce^{IV} ions are eight coordinate and in square antiprismatic {CeO_8} geometries. The addition of NH_4ClO_4 to the reaction seems critical to the formation of **35** even though neither cation or anion is incorporated into the cluster. Repeating the reaction that produced **34** but using $DyCl_3{\cdot}6H_2O$ in a basic dmf/MeOH solvent combination and under solvothermal conditions (T = 130 °C, 24 h) results in the formation of $[Dy^{III}_7O_2(OH)_4(H_1TBC[8])(H_2TBC[8])(dmf)_9]$ (**36**; Fig. S17, ESI†).[34] The metallic skeleton of **36** describes a distorted, capped octahedron. The central cavity is again occupied by two μ_4-O^{2-} ions, with the capping Dy^{III} ion connected to the octahedron through a combination of two μ_3-OH^- ions and one μ-OH^- ion. The remaining OH^- ion μ-bridges between two Dy^{III} ions in the square plane of the octahedron. The two calix[8]arene ligands are mono- and doubly deprotonated, respectively. In the former the single proton is shared between neighbouring O(Ph) atoms, both of which are terminally coordinated. This ligand bridges a total of six Dy^{III} ions. For the latter, the two protonated arms are bonded terminally with very large Dy···O distances. This ligand bridges a total of five Dy^{III} ions. The Dy^{III} ions are of two types: eight coordinate and in square antiprismatic {LnO_8} geometries, or seven coordinate and in pentagonal bipyramidal {LnO_7} geometries. The remaining metal coordination sites are filled with terminally bonded dmf molecules. The magnetic properties of **32**, **34** and **36** were not reported.

The final Dy-based cluster reported is the complex $[NaDy^{III}(H_6TBC[8])(OAc)_2(dmf)_3]$ (**37**; Fig. S18, ESI†), made from the reaction of $Dy(OAc)_3{\cdot}6H_2O$, $H_8TBC[8]$, 1,1,1-tris(hydroxymethyl) ethane ($thmeH_3$) and NEt_3 in dmf/ethyl acetate (Fig. S18, ESI†).[35] The doubly deprotonated $H_6TBC[8]$ ligand adopts the pleated-loop conformation, with the two neighbouring deprotonated O(Ph) atoms chelating the Dy ion. The two OAc^- ligands also chelate to the Dy ion, using one O atom to μ-bridge to the Na ion. The coordination geometry of the Dy is completed with one molecule of dmf. The resulting {DyO_8} environment is best described as distorted triangular dodecahedron. The Na ion is five-coordinate and has a distorted square pyramidal {NaO_5} geometry, the remaining bonds comprising one molecule of dmf and two neighbouring, protonated O(Ph) atoms from the calix[8]arene. Interestingly, the {NaDy} lies outwith the $H_6TBC[8]$ plane, perhaps due to the bridging acetates being located on the same side of the {NaDy} dimer. The role of the $thmeH_3$ ligand in the reaction is unclear, but its addition appears necessary for the isolation of the product. Complex **37** is a field induced SMM, albeit with a very small U_{eff} value.[35]

Replacing $DyCl_3{\cdot}6H_2O$ with $GdCl_3{\cdot}6H_2O$ in an otherwise identical reaction to that which produces **36** leads to the isolation of the complex $[Gd^{III}_8(H_1TBC[8])_2(CO_3)_4(HCOO)_2(dmf)_8]$ (**38**; Fig. 19).[34] The metallic skeleton of **38** conforms to the 26th Johnson solid (J_{26}), the gyrobifastigium. This 8-vertex polyhedron is composed of four squares and four triangles constructed around a central square plane. It is perhaps best envisioned as two triangular prisms sharing a square face, with one prism given a quarter-turn.

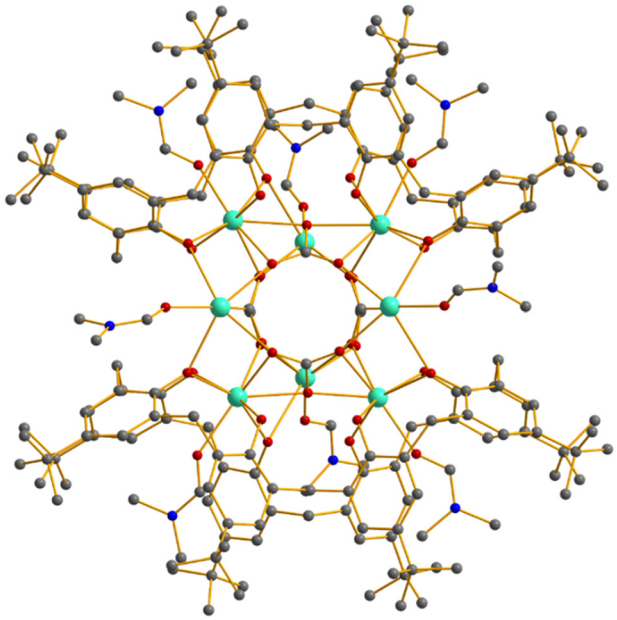

Fig. 19 The structure of the cation of compound **38**. Colour code: Gd = cyan, O = red, N = blue, C = grey. H atoms omitted for clarity.

The metallic core is held together by a combination of two μ_5-CO_3^{2-}, three μ_4-CO_3^{2-} and two *syn, syn*, μ-$HCOO^-$ ligands. The CO_3^{2-} and $HCOO^-$ ligands are derived from the fixation of atmospheric CO_2 and the oxidation of MeOH, respectively. Both are commonly observed in Ln cluster chemistry, and especially so under solvothermal (high temperature, high pressure) reaction conditions.[36] The two calix[8]arenes sandwich the inorganic core of the complex and are singly protonated, $H_1TBC[8]$, the proton being shared between O(Ph) neighbours which are all are terminally coordinated. Each ligand bonds to a total of five Gd centres, all being seven coordinate and in distorted pentagonal bipyramidal {GdO_7} geometries. It is interesting to note that complex **38** contains no O^{2-}/OH^- ions, in contrast to **33–36** despite the similarities in synthetic methodologies. It is also clear the that CO_3^{2-} ions generated *in situ* have acted as their ''replacement''. In turn, this suggests that deliberately incorporating carbonate ions into this chemistry (and other Ln chemistry) would be a fruitful source of new complexes.[36] The magnetic properties of **38** were not reported.

By far the largest Ln-based cluster reported is $[Ln^{III}_{18}O_3(OH)_{12}(TBC[8])_3(CO_3)_2Cl_6(H_2O)_6(dmf)_{18}Cl]OH$ (Ln = La (**39a**), Nd = (**39b**), Gd = (**39c**); Fig. 20), made from the reaction of $[Ln^{III}_2(H_2TBC[8])(DMSO)_3(H_2O)]$ with trimesic acid in a basic $CHCl_3$/dmf/MeOH solution under solvothermal conditions (120 °C, 48 hrs).[37] The metallic skeleton of **39** describes an intercalated trigonal prism and an irregular polyhedron that consists of six equilateral triangles and eight isosceles trapezia. This framework is templated by a single Cl^- anion that sits in the centre of the cage. Twelve μ_3-OH^- ions, six μ_3-Cl^- ions, three μ_4-O^{2-} ions and two μ_3-CO_3^{2-} ions connect the Ln^{III} ions together in the core of the molecule. The cationic cluster has D_{3h} (trigonal planar) symmetry with the C_3 axis passing through the two central C-atoms of the CO_3^{2-} ligands.

This journal is © The Royal Society of Chemistry 2025

Open Access Article. Published on 22 2024. Downloaded on 31.05.2026 00:39:47.
This article is licensed under a Creative Commons Attribution-NonCommercial 3.0 Unported Licence.

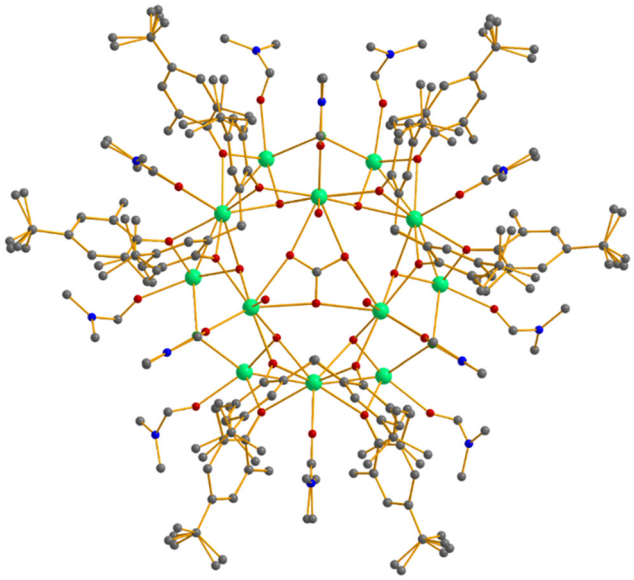

Fig. 20 The structure of the cation of compound **39**. Colour code: Ln = light green, O = red, N = blue, C = grey, Cl = yellow. H atoms omitted for clarity.

The three fully deprotonated TBC[8] ligands sit on the three triangular vertices, fully encapsulating the inorganic core and adopt the double-cone conformation. All eight O(Ph) atoms μ-bridge between neighbouring Ln^{III} ions. The remaining coordination sites on the Ln^{III} ions are occupied by terminally bonded H_2O and dmf molecules. The three unique Ln^{III} ions in the ASU unit adopt distorted square antiprismatic $\{LnO_8\}$, distorted square antiprismatic $\{LnO_6Cl_2\}$, and distorted capped square antiprismatic $\{LnO_8Cl\}$ geometries. The OH^- counter anion is H-bonded to three coordinated water molecules that sit on one of the triangular $\{Ln_3\}$ faces of the cluster. The release of Cl^-/CO_3^{2-} ions during the reaction is clearly essential for the construction of the complex. These originate from the dehalogenation of $CHCl_3$/fixation of atmospheric CO_2. Although not incorporated into the structure, the addition of trimesic acid also appears to be vital as repetitions of the reaction without it fail to produce **39**. The authors suggested that its presence in the reaction mixture may prevent the isolation of smaller TBC[8]-based Ln complexes.[37]

The magnetic properties of **39b** (Nd analogue) and **39c** (Gd analogue) are dominated by the presence of very weak antiferromagnetic exchange interactions, with a Curie–Weiss constant, $\theta = -3.1$ K for **39c**. This was corroborated by heat capacity (c_p) measurements in which the zero-field magnetic contribution to c_p is nicely simulated by a Schottky model for eighteen $S = 7/2$ spins and an effective magnetic field $B_{eff} = 0.6$ T that mimics the magnetic interactions, $g\mu_B SB_{eff} = 2.8\ \text{K} \approx |\theta|$, for $g = 2.0$.

Summary of Ln-based clusters

An inspection of the metallic skeletons of the Ln-based complexes reveals the prevalence of dimeric $\{Ln_2\}$ species and clusters based on octahedra or the component parts of octahedra – capped triangles, square-based pyramids, capped octahedra. For example, a simple comparison of Fig. 18–20 highlights some significant similarities. Calix[8]arene ligands have proven to be excellent scaffolds for the oxophilic Ln^{III} ions, and this is reflected in the number of homo- and heterometallic species isolated. They display a variety of conformations and a range of deprotonation levels. Unsurprisingly, the size/nuclearity of these species appears to be directly related to the deprotonation level of the ligand. Interestingly, however, there remains only six homometallic clusters with a nuclearity of four or more, $\{Ce^{IV}_4\}$, $\{Tb^{III}_5\}$, $\{Ce^{IV}_6\}$, $\{Dy^{III}_7\}$, $\{Gd^{III}_8\}$ and $\{Ln^{III}_{18}\}$. The latter was made *via* a tandem templating strategy and a dimeric $\{Ln_2\}$ starting material, perhaps pointing towards a method for constructing larger species. Given the general preference of TBC[4]-supported Ln^{III} ions to form octahedra, the combination of both H_4TBC[4] and H_8TBC[8] in the same reaction may prove to be complementary. Likewise, heterometallic 4f species, *e.g.* Ce^{IV} and Gd^{III}, may lead to some interesting discoveries.

Given that V-based TBC[8]-supported clusters have found utility in catalysis,[8–13] Ln-based species may also be of interest from that perspective. For example, complex **31** is monometallic and the assembly itself is in a chiral conformation.[33] Although it would require resolution of this species, if achieved, this would have potential utility in catalysis, as may other larger polymetallic Ln-based clusters.

Although not covered in this review (given the focus on structural and magnetic properties), it is worth noting that Ln-based calixarene complexes have fascinating luminescent properties which can be tuned/manipulated through synthetic alteration of the C[*n*] framework. A relatively recent review by Massi and Ogden highlights the antenna effect calixarenes can provide in such complexes, but also covers early work in which the photophysical properties of compound **30** in detail.[38] The Ln-based systems covered herein should be revisited to study such properties in detail, and indeed any further examples isolated should be studied to provide greater insight into how these species may be incorporated into materials, for example.

Conclusions

Systematic exploration of the coordination chemistry of H_4TBC[4] previously allowed us to establish a series of empirical metal ion binding rules that also translate very effectively to H_8-bis-TBC[4].[1,3] Coordination chemistry is promoted by the common cone conformation adopted by C[4]s, and this may benefit from synthetic modification at the methylene bridge positions in future as this (in principle) does not interfere with the polyphenolic pocket. The larger, odd-numbered homologues of H_4TBC[4] hold enormous potential for application in the synthesis of coordination clusters. However, greatly improved synthetic protocols are required for H_nTBC[*n*] where *n* is 7 or 9 as these would need to be scaled up for exploratory cluster synthesis with a wide range of 3d and 4f ions. In this review we have shown that, to date, a large number of clusters

Open Access Article. Published on 22 2024. Downloaded on 31.05.2026 00:39:47.
This article is licensed under a Creative Commons Attribution-NonCommercial 3.0 Unported Licence.

formed using H_8TBC[8] as a ligand have been synthesised. Interestingly, only a relatively small number have been prepared using benchtop or solvothermal conditions. The varying degrees of deprotonation possible in H_8TBC[8], coupled with the ability to form homo/heterometallic assemblies, suggests that a systematic study of the associated coordination chemistry of this ligand will unearth a huge number of new polymetallic clusters. For example, one only has to compare the Mn complexes of H_4TBC[4] with those formed with H_8TBC[8] to identify an area worthy of further investigation. Indeed, a systematic study of the entire 3d series is warranted. Such studies would ideally afford a set of empirical ion binding rules akin to those for H_4TBC[4] that, once in hand, could potentially be used to target hetero-calixarene assemblies, *i.e.* systems supported by both ligand types that display their own structural preferences. Inspection of the clusters reported herein already delivers some structural trends, *e.g.* a tendency towards dimers, butterflies and octahedra. Fig. S19–S24 (ESI†) collect all the metallic skeletons of the polymetallic complexes reported herein for comparison. Formation of the very large Ln_{18} cluster suggests that it may be possible to access even larger assemblies that conform to highly symmetric solids capped by TBC[8]s in the double-cone conformation; this would be a direct extension from the well-documented structure-capping behaviour of TBC[4].

From a synthetic standpoint, a systematic exploration of the coordination chemistry of any chosen H_nTBC[n] should carefully examine the role of solvothermal conditions in the clusters that result from this chemistry. This synthetic approach clearly has the capability to deliver fascinating new species,[37] but achieving a far greater understanding of the influence of these conditions over the calixarene (cluster support) and components that are found in the products will be vital to (a) compiling a set of binding rules for any particular H_nTBC[n], and (b) tailoring the formation of desirable assemblies.

A broad review of coordination chemistry of the larger calixarenes by Redshaw in 2003 demonstrated how the field had developed to that point, identifying a wide range of potential routes of investigation.[39] Despite the number of species covered in this review, the coordination chemistry of H_8TBC[8] may still be considered embryonic. Work in our labs has begun a systematic study of the 3d and 4f ions, the results from which will be reported in due course. Ready access to other large(r), odd and even-numbered H_nTBC[n]s on a useable scale will also be pursued, as these ligands offer fascinating opportunities depending on ring size, preferred conformations, *etc.* However, it does not always follow that larger ligands will deliver larger clusters, an example being that H_{16}TBC[16] adopts a pseudo-spherical conformation in the solid state due to folding and ring size (with phenolic groups all pointing inwards).[40] This feature may hinder large cluster formation, so one must consider many factors when attempting to systematically programme the assembly of such complex systems. Nevertheless, calix[n]arene coordination chemistry remains a fascinating area for scientific exploration, and we hope this review stimulates activity in the area.

Data availability

No primary research results, software or code have been included and no new data were generated or analysed as part of this review.

Conflicts of interest

There are no conflicts to declare.

Acknowledgements

EKB and SJD thank the EPSRC for funding grants EP/I031421/1 & EP/I03255X/1. EKB thanks the Leverhulme Trust (RPG-2021-176).

Notes and references

1 L. R. B. Wilson, M. Coletta, M. Evangelisiti, S. Piligkos, S. J. Dalgarno and E. K. Brechin, *Dalton Trans.*, 2022, **51**, 4213, and references therein.
2 I. Thondorf, *Chapter 15 in Calixarenes 2001*, ed. Z. Asfari, C. Böhmer, J. Harrowfield, J. Vicens, Kluwer Academic Publishers, Dordrecht, 2001.
3 I. V. Khariushin, V. Bulach, S. E. Solovieva, I. S. Antipin, A. S. Ovsyannikov and S. Ferlay, *Coord. Chem. Rev.*, 2024, **513**, 215846.
4 S. Fleming, C. D. Gutsche, J. M. Harrowfield, M. I. Ogden, B. W. Skelton, D. G. Stewart and A. H. White, *Dalton Trans.*, 2003, 3319, and references therein.
5 M. Coletta, E. K. Brechin and S. J. Dalgarno, in *Chapter 25 in Calixarenes and Beyond*, ed. P. Neri, J. L. Sessler and M.-X. Wang, Springer Nature, Switzerland, 2016.
6 A. Kieliszek and M. Malinska, *Cryst. Growth Des.*, 2021, **21**, 6862, and references therein.
7 J. L. Atwood, G. A. Koutsantonis and C. L. Raston, *Nature*, 1994, **368**, 229; T. Suzuki, K. Nakashima and S. Shinkai, *Tet. Lett.*, 1995, **36**, 249; X. Chen, R. A. Boulos, A. D. Slattery, J. L. Atwood and C. L. Raston, *Chem. Commun.*, 2015, **51**, 11413.
8 G. E. Hofmeister, E. Alvarado, J. A. Leary, D. I. Yoon and S. F. Pedersen, *J. Am. Chem. Soc.*, 1990, **112**, 8843.
9 V. C. Gibson, C. Redshaw and M. R. J. Elsegood, *J. Chem. Soc., Dalton Trans.*, 2001, 767.
10 E. Hoppe, C. Limberg and B. Ziemer, *Inorg. Chem.*, 2006, **45**, 8308.
11 C. Redshaw, M. J. Walton, D. S. Lee, C. Jiang, M. R. J. Elsegood and K. Michiue, *Chem. – Eur. J.*, 2015, **21**, 5199.
12 T. Xing, M. Derbyshire, M. R. J. Elsegood and C. Redshaw, *Chem. Commun.*, 2022, **58**, 7427.
13 A. Ignaszak, N. Patterson, M. Radtke, M. R. J. Elsegood, J. W. A. Frese, J. L. Z. F. Lipman, T. Yamato, S. Sanz, E. K. Brechin, T. J. Prior and C. Redshaw, *Dalton Trans.*, 2018, **47**, 15983.
14 S. Petit, G. Pilet, D. Luneau, L. F. Chibotaru and L. Ungur, *Dalton Trans.*, 2007, 4582.
15 S. C. Du, Y. F. Bi, Y. Yu and W. Liao, *Sci. Sin.: Chim.*, 2012, **42**, 1356.
16 H. Han, X.-L. Li, X. Zhu, G. Zhang, X. Hang, J. Tang and W. Liao, *Eur. J. Inorg. Chem.*, 2017, 4879.
17 H. Han., Y.-S. Ding, X. Zhu, T. Han, Y.-Z. Zheng and W. Liao, *Inorg. Chem. Front.*, 2020, **7**, 4070.
18 S.-C. Du, H.-Q. Tan, Y.-F. Bi, Y. Yu and W.-P. Liao, *Chin. J. Inorg. Chem.*, 2014, **30**, 749.
19 A. Ignaszak, N. Patterson, C. O'Brien, A. True, M. R. J. Elsegood, T. J. Prior and C. Redshaw, *RSC Adv.*, 2022, **12**, 11672.
20 R. A. Green, A. L. Rheingold and C. S. Weinert, *Inorg. Chim. Acta*, 2009, **362**, 3159.
21 A. E. Wetherby, L. R. Goeller, A. G. DiPasquale, A. L. Rheingold and C. S. Weinert, *Inorg. Chem.*, 2007, **46**, 7579.
22 A. Arbaoui, C. Redshaw, M. R. J. Elsegood, V. E. Wright, A. Yoshizawa and T. Yamato, *Chem. – Asian J.*, 2010, **5**, 621.
23 R. D. McIntosh, S. M. Taylor, S. Sanz, C. M. Beavers, S. J. Teat, E. K. Brechin and S. J. Dalgarno, *Dalton Trans.*, 2011, **40**, 12265;

 This journal is © The Royal Society of Chemistry 2025

Open Access Article. Published on 22 2024. Downloaded on 31.05.2026 00:39:47.
This article is licensed under a Creative Commons Attribution-NonCommercial 3.0 Unported Licence.

A. R. E. Baikie, A. J. Howes, M. B. Hursthouse, A. B. Quick and P. Thornton, *J. Chem. Soc., Chem. Commun.*, 1986, 1587.
24 R. McLellan, S. M. Taylor, R. D. McIntosh, E. K. Brechin and S. J. Dalgarno, *Dalton Trans.*, 2013, **42**, 6697.
25 S. Du, H. Ke, Y. Bi, H. Tan, Y. Yu, J. Tang and W. Liao, *Inorg. Chem. Commun.*, 2013, **29**, 85.
26 G. Karotsis, S. J. Teat, W. Wernsdorfer, S. Piligkos, S. J. Dalgarno and E. K. Brechin, *Angew. Chem., Int. Ed.*, 2009, **48**, 8285; S. M. Taylor, G. Karotsis, R. D. McIntosh, S. Kennedy, S. J. Teat, C. M. Beavers, W. Wernsdorfer, S. Piligkos, S. J. Dalgarno and E. K. Brechin, *Chem. – Eur. J.*, 2011, **17**, 7521; M. A. Palacios, R. McLellan, C. M. Beavers, S. J. Teat, H. Weihe, S. Piligkos, S. J. Dalgarno and E. K. Brechin, *Chem. – Eur. J.*, 2015, **21**, 11212; S. M. Taylor, R. D. McIntosh, C. M. Beavers, S. J. Teat, S. Piligkos, S. J. Dalgarno and E. K. Brechin, *Chem. Commun.*, 2011, **47**, 1440; S. M. Taylor, J. M. Frost, R. McLellan, R. D. McIntosh, E. K. Brechin and S. J. Dalgarno, *CrystEngComm*, 2014, **16**, 8098; S. M. Taylor, R. D. McIntosh, S. Piligkos, S. J. Dalgarno and E. K. Brechin, *Chem. Commun.*, 2012, **48**, 11190; R. McLellan, M. A. Palacios, S. Sanz, E. K. Brechin and S. J. Dalgarno, *Inorg. Chem.*, 2017, **56**, 10044; G. Karotsis, S. Kennedy, S. J. Dalgarno and E. K. Brechin, *Chem. Commun.*, 2010, **46**, 3884.
27 H. Han, X. Li, X. Zhu, G. Zhang, S. Wang, X. Hang, J. Tang and W. Liao, *Eur. J. Inorg. Chem.*, 2017, 2088.
28 B. M. Furphy, J. M. Harrowfield, D. L. Kepert, B. W. Skelton, A. H. White and F. R. Wilner, *Inorg. Chem.*, 1987, **26**, 4233.
29 J. M. Harrowfield, M. I. Ogden and A. H. White and F. R. Wilner, *Aust. J. Chem.*, 1989, **42**, 949.
30 J. M. Harrowfield, M. I. Ogden and A. H. White, *Aust. J. Chem.*, 1991, **44**, 1237.
31 J. M. Harrowfield, M. I. Ogden and A. H. White, *Aust. J. Chem.*, 1991, **44**, 1249.
32 J.-C. G. Bünzli, F. Ihringer, P. Dumy, C. Sager and R. D. Rogers, *J. Chem. Soc., Dalton Trans.*, 1998, 497.
33 J. M. Harrowfield, M. I. Ogden, W. R. Richmond and A. H. White, *J. Chem. Soc., Dalton Trans.*, 1991, 2153.
34 S. M. Taylor, S. Sanz, R. D. McIntosh, C. M. Beavers, S. J. Teat, E. K. Brechin and S. J. Dalgarno, *Chem. Eur. J.*, 2012, **18**, 16014.
35 H.-S. Wang, Y. Chen, Z.-B. Hu, Q.-Q. Long, C.-L. Yin, Z.-C. Zhang and Z.-Q. Pan, *Inorg. Chem. Commun.*, 2019, **105**, 76.
36 L. Natarajan, J. Pecaut and M. Mazzanti, *Dalton Trans.*, 2006, 1002; P. C. Andrews, T. Beck, C. M. Forsyth, B. H. Fraser, P. C. Junk, W. Massi and P. W. Roesky, *Dalton Trans.*, 2007, 5651; X.-L. Tang, W.-H. Wang, W. Dou, J. Jiang, W.-S. Liu, W.-W. Qin, G.-L. Zhang, K.-B. Yu and L.-M. Zheng, *Angew. Chem., Int. Ed.*, 2009, **48**, 3499; T. N. Hooper, R. Inglis, M. A. Palacios, G. S. Nichol, M. B. Pitak, S. J. Coles, G. Lorusso, M. Evangelist and E. K. Brechin, *Chem. Commun.*, 2014, **50**, 3498.
37 Y. Jiao, S. Sanz, J. van Leusen, D. Gracia, A. B. Canaj, M. Evangelisti, E. K. Brechin, S. J. Dalgarno and P. Kögerler, *Dalton Trans.*, 2024, **53**, 4624.
38 M. Massi and M. Ogden, *Materials*, 2017, **10**, 1369.
39 C. Redshaw, *Coord. Chem. Rev.*, 2003, **244**, 45.
40 C. Bavoux, R. Baudry, I. Dumazet-Bonnamour, R. Lamartine and M. Perrin, *J. Inclusion Phenom. Macrocyclic Chem.*, 2001, **40**, 221.